



Universiteit
Leiden
The Netherlands

The effects of breast cancer therapy on estrogen receptor signaling throughout the body

Droog, M.

Citation

Droog, M. (2017, June 8). *The effects of breast cancer therapy on estrogen receptor signaling throughout the body*. Retrieved from <https://hdl.handle.net/1887/49509>

Version: Not Applicable (or Unknown)

License: [Licence agreement concerning inclusion of doctoral thesis in the Institutional Repository of the University of Leiden](#)

Downloaded from: <https://hdl.handle.net/1887/49509>

Note: To cite this publication please use the final published version (if applicable).

Cover Page



Universiteit Leiden



The handle <http://hdl.handle.net/1887/49509> holds various files of this Leiden University dissertation

Author: Droog, Marjolein

Title: The effects of breast cancer therapy on estrogen receptor signaling throughout the body

Issue Date: 2017-06-08

Chapter 4

Phosphorylation of Activating Transcription Factor-2 (ATF-2) within the Activation Domain is a Key Determinant of Sensitivity to Tamoxifen in Breast Cancer

Bharath Rudraraju, Marjolein Droog*, Tarek M. A. Abdel-Fatah*, Wilbert Zwart, Athina Giannoudis, Mohammed I. Malki, David Moore, Hetal Patel, Jacqui Shaw, Ian O. Ellis, Steve Chan, Greg N. Brooke, Ekaterina Nevedomskaya, Christiana Lo Nigro, Jason Carroll, R. Charles Coombes, Charlotte Bevan, Simak Ali, Carlo Palmieri

* equal contribution

Breast Cancer Res Treat 147 (2014) 295-309

Abstract

Activating transcription factor-2 (ATF-2) has been implicated as a tumour suppressor in breast cancer (BC). c-JUN N-terminal kinase (JNK) and p38 MAPK phosphorylate ATF-2 within the activation domain (AD), which is required for its transcriptional activity. To date, the role of ATF-2 in determining response to endocrine therapy has not been explored. Effects of ATF-2 loss in the oestrogen receptor (ER)-positive luminal BC cell line MCF-7 were explored, as well as its role in response to tamoxifen treatment. Genome-wide chromatin binding patterns of ATF-2 when phosphorylated within the AD in MCF-7 cells were determined using ChIP-seq. The expression of ATF-2 and phosphorylated ATF-2 (pATF-2-Thr71) was determined in a series of 1,650 BC patients and correlated with clinico-pathological features and clinical outcome. Loss of ATF-2 diminished the growth-inhibitory effects of tamoxifen, while tamoxifen treatment induced ATF-2 phosphorylation within the AD, to regulate the expression of a set of 227 genes for proximal phospho-ATF-2 binding, involved in cell development, assembly and survival. Low expression of both ATF-2 and pATF-2-Thr71 was significantly associated with aggressive pathological features. Furthermore, pATF-2 was associated with both p-p38 and pJNK1/2 (< 0.0001). While expression of ATF-2 is not associated with outcome, pATF-2 is associated with longer disease-free ($p = 0.002$) and BC-specific survival in patients exposed to tamoxifen ($p = 0.01$). Furthermore, multivariate analysis confirmed pATF-2-Thr71 as an independent prognostic factor. ATF-2 is important for modulating the effect of tamoxifen and phosphorylation of ATF-2 within the AD at Thr71 predicts for improved outcome for ER-positive BC receiving tamoxifen.

Abbreviations

AD, activation domain; AR, androgen receptor; ATM, ataxia telangiectasia mutated; ATF-2, activating transcription factor-2 ; BC, breast cancer; BCSS, breast cancer-specific survival; CK, cytokeratin; CRE, ATF/cAMP-response elements ; DFS, Disease-free survival; EMT, epithelial-mesenchymal transition; ER, oestrogen receptor; HR, hazard ratio; IDC-NST, invasive ductal no special type; IHC, immunohistochemistry; JNK,c-JUN N-terminal kinase; MEFs, mouse embryonic fibroblasts; NFY, nuclear transcription factor Y; NR1I2, nuclear receptor subfamily 1, group 1, member 2; NR4A1, nuclear receptor subfamily 4, group A, member 1; pATF-2-Thr71, phosphorylated ATF-2 ; PKC, protein kinase C; PLAG1, pleiomorphic adenoma gene 1; PR, progesterone receptor; SMA, smooth muscle actin; SRB, sulphorhodamine B.

Introduction

Expression of oestrogen receptor alpha (herein called ER α) predicts for response to endocrine therapy¹, and adjuvant endocrine therapy improves survival in ER α -positive breast cancer². However, resistance, *de novo* or acquired, limits the use of endocrine therapy³. Understanding the underlying molecular mechanisms that mediate resistance is required to improve management of endocrine resistant breast cancer, and to facilitate the development of novel therapeutic strategies⁴.

Activating transcription factor-2 (ATF-2) is a member of the ATF and CREB group of bZIP transcription factors⁵. ATF-2 regulates gene transcription by forming homodimers but also functions as heterodimers with other ATF family members⁶ and AP-1 family members⁷. These homo- and hetero-dimers bind to ATF/cAMP-response elements (CRE)^{8,9} where they dictate transcriptional control, chromatin remodelling and the response to DNA damage¹⁰⁻¹². Phosphorylation events at two threonine residues, Thr69 and Thr71, within the activation domain (AD) of ATF-2 are required to stimulate its transcriptional activity¹³⁻¹⁵. c-JUN N-terminal kinase (JNK) and p38 MAPK phosphorylate both Thr69 and Thr71¹⁴⁻¹⁶, while mitogens such as EGF via ERK1/2 induce phosphorylation of Thr71 alone¹⁷. The role of Ser90, also located within the AD, is unclear^{18,19}. Several other ATF-2 phosphorylation sites have been identified, including Ser121, Ser340 and Ser367, which are phosphorylated by protein kinase C (PKC)^{20,21}, while ataxia telangiectasia mutated (ATM) phosphorylates Ser490 and Ser498²².

The potential importance of ATF-2 phosphorylation in breast cancer has been shown by p38-mediated phosphorylation increasing ATF-2 binding to the CRE in the cyclin D1 promoter following growth factor treatment²³, as well as activation of the AP-1 site of MMP-2 with induction of invasive and migration phenotypes²⁴. It has also been reported that estradiol and its metabolites 16-hydroxyestrone enhanced the DNA-binding activity of ATF-2 to the cyclin D1 CRE/ATF site, while 2-methoxyestradiol blocked this process²⁵. Furthermore, JNK-dependent phosphorylation of ATF-2 promotes resistance to DNA damaging agents in the context of a HER2-overexpressing breast cancer cell line²⁶, with subsequent chromatin immunoprecipitation (ChIP) of ATF-2 revealing the largest functional group of genes activated by JNK are those involved in DNA repair²⁷.

ATF-2 has been reported to have tumour suppressor properties in breast cancer with heterozygous ATF-2 knockout (atf2 +/-) mice predisposed to developing mammary tumours²⁸. Furthermore, ATF-2 is required for the induction of FOXP3 and FOXP3-mediated apoptosis in the context of murine mammary cancer²⁹. In human breast cancer, ATF-2 mRNA levels were lower as compared to the normal mammary gland²⁸. While a study of ATF-2 expression in 134 human breast cancers gave varying results depending on the reagents and methodology used³⁰. High ATF-2

protein expression measured by immunoblotting and immunohistochemistry (IHC) was associated with a shorter overall survival. However, high phosphorylation of ATF-2 at Thr69 and Thr71 (pATF-2-Thr69/pThr71) as measured by immunoblotting correlated with a well-differentiated phenotype, but not with prognosis, while increased levels of pThr69-ATF-2 by immunohistochemistry were associated with prolonged survival³⁰.

In the current study, we sought to investigate the role of ATF-2 and phosphorylation within the AD in mediating the anti-tumour activity of tamoxifen and its use as a marker for predicting response to endocrine therapy.

Materials and Methods

Breast Cancer Cell Lines

MCF-7 cells were obtained from the Cancer Research UK Cell services (Clare Hall Laboratories, South Mimms, Herts, UK) and maintained in Dulbecco's Modified Eagle Medium (DMEM) supplemented with 10 % foetal bovine serum, 5 mM L-glutamine and 1 % penicillin/streptomycin.

siRNA, Transfections, Nucleic Acid Isolation and RT-PCR Analysis

Cells were transfected using Lipofectamine RNAiMAX, according to manufacturer's methods (Invitrogen, Paisley, UK). RNA and protein were prepared 48 h following transfection. Cell number was determined using the sulphorhodamine B (SRB) growth assay, as described previously³¹, and colony formation was assessed by plating the cells in soft agar for 21 days as described in supplementary methods. Plates were scanned, and the colonies were counted using an Optronix Gel Count (Oxford Optronix, UK).

ON-TARGET plus SMARTpool siRNA, Human ATF-2 (see below for details) and ON-TARGET plus Non-targeting Control Pool Catalogue number D-001810-10-20 (ABgene Ltd, Surrey, UK) were used for ATF-2 knockdown experiments. ON-TARGET plus SMARTpool, Human ATF-2, Catalogue number, L-009871-00-0010, ORF (ABgene Ltd, Surrey, UK) with following sequences were used:

- (1) GAGAAGAGCAGCUAACGAA
- (2) CAUGGUAGCGGAUUGGUUA
- (3) GGAAGUACCAUUGGCACAA
- (4) UGAGGAGCCUUCUGUUGUA

RNA isolation, cDNA preparation and RT-PCR were performed as described in supplementary information.

Re-expression of ATF-2 using plasmid pact1-ATF-2 (kind gift of T. Maekawa, S Ishii, RIKEN, Japan) was performed using Fugene 6 at a 1:3 ratio (Roche, Diagnostics, Burgess Hill, UK) following manufacturer's protocol. Briefly, after 48 h, siATF-2 cells were transfected using 1 µg of ATF-2 plasmid. One day after transfection, media was changed to vehicle only and tamoxifen. SRB assay was performed as before.

Immunoblotting

After ATF-2 knockdown using siRNA, cell lysates were prepared in RIPA buffer (Sigma-Aldrich Company Ltd, Gillingham, UK) with protease and phosphatase inhibitors (Roche Diagnostics, Burgess Hill, UK). For experiments in which 4-hydroxytamoxifen was added, cells were cultured in DMEM lacking phenol red and containing 10 % charcoal stripped foetal calf serum for 48 h prior to treatment, and lysates were prepared in RIPA buffer, and immunoblotting was performed.

Following immunoblotting, membranes were probed with antibodies overnight; after washing and incubation with secondary antibody, they were developed with Supersignal West Pico Chemiluminescent Substrate (VWR International Ltd, Lutterworth, UK). Images were captured on the UVitec Cambridge Image Reader using the Alliance 2.7 software, and densitometry was performed by the AIDA/2D v4.27 analysis software.

Antibodies were applied targeting ER (Vector Laboratories, Peterborough, UK), JNK1/2, pJNK1/2 (phospho-Thr183/Tyr185), ERK1/2, pERK1/2 (phospho-Thr202/Tyr204) and pATF-2 (phospho-Thr69/71 and Thr71) (all from New England Biolabs, Hertfordshire, UK). p38 and p-p38 MAPK (phospho-Thr180/Tyr182), ATF-2 and α -tubulin were purchased from Insight Biotechnology, Middlesex, UK, and Secondary horseradish peroxidase-conjugated antibodies were from Dako UK Ltd, Cambridgeshire, UK

Chromatin Immuno Precipitation and Solexa Sequencing (ChIP-Seq)

Exponentially growing MCF-7 cells were treated with 100nM 4-OH Tamoxifen for 1 hour, and cells were fixed, chromatin was isolated, and CHIP was performed (see supplementary information).

Motif Analysis, Heatmaps, Genomic Distributions of Binding Events and in silico Survival Analyses

ChIP-seq data snapshots were generated using the integrative genome viewer IGV 2.2 (www.broadinstitute.org/igv). Genomic analyses and Motif enrichment analyses were performed using the Cistrome (cistrome.org), applying the SeqPos motif tool³². For analysis information, see supplementary information.

The prognostic potential of the genes with proximal ATF-2 binding was assessed using two publicly available gene expression datasets with GEO accession numbers GSE6532³³ and GSE2034³⁴. Genes with a pATF-2-Thr71 binding site within a 20 kb window from their transcription start site (TSS) were analysed. Hierarchical clustering of the gene expression was performed using correlation as a distance measure and average linkage. Groups of patients were defined based on the two biggest clusters in the hierarchical clustering. The Cox proportional hazards model was used to compute the hazard ratio (HR) in the analysis of time to relapse or to distant metastasis. Survival curves were generated using the Kaplan–Meier method, and a log-rank test was used to test for differences. All the analyses were performed using R statistical software.

Paired Primary and Secondary Breast Cancers

Twenty primary breast carcinomas with a paired metastasis as well as normal controls from reduction mammoplasty were acquired from the pathology archives of S Croce General Hospital, Cuneo, Italy (See supplementary information).

Nottingham Tenovus Primary Breast Cancer Series

Primary operable breast cancer cases ($n = 1650$) from the Nottingham Tenovus Primary Breast Carcinoma Series were used^{35,36}, and were utilised for immunohistochemistry (see supplementary information). Clinical data were maintained on a prospective basis with a median follow-up of 126 months (range 4–247).

Immunohistochemistry

The tissue microarrays and full-face sections from the Nottingham Tenovus Primary breast cancer series were immunohistochemically profiled for ATF-2, pATF-2-Thr71 and other biological antibodies as previously described³⁷. ATF-2 rabbit polyclonal antibody was directed against amino acids 1-96 (Santa Cruz, Heidelberg, Germany), and phospho-Thr71 ATF-2 polyclonal rabbit antibody (Cell signalling technology, Danvers, USA) was

optimised to a working concentration, utilizing 4 μm full-face excisional tissue sections.

Antigen retrieval was performed using citrate buffer (pH 6.0) and microwave heating (20 min at 750 Watts). Subsequently, 4 μm TMA sections were immuno-stained using the optimised staining protocol. Detection was achieved using the Novalink Polymer Detection kit (Leica Microsystems Inc., USA). Negative controls were performed by omission of the primary antibody.

IHC revealed that ATF-2 and pATF-2-T71 had a nuclear location (Supplementary Figure S6). Nuclear staining was scored based on the H-score and Allred Quick score, and the median H-score was 123 for ATF-2 (interquartile range, 0–270) and 92.5 for pATF-2 (interquartile range, 0–272). For all subsequent analyses, ATF-2 expression was categorized as low/loss if the H-score < 123, while pATF-2-pT71 expression was categorized as low/loss if the Quick score < 6. Determination of the optimal cut-offs was performed using histograms and confirmed using X-tile bioinformatics software (Yale University, USA) where data were split into training and validation sets. A total of 1,516 and 1,388 tumours were suitable for analysis of both pATF-2-pT71 and ATF-2, respectively.

To validate the use of TMAs for immuno-phenotyping in the group treated with primary surgery, full-face sections of 40 cases were stained, and the protein expression levels of the different antibodies were compared. The concordance between TMAs and full-face sections was excellent ($\kappa = 0.8$). Positive and negative (omission of the primary antibody and IgG-matched serum) controls were included in each run. The tumour cores were evaluated by three of coauthors (TMA-F, IOE and DM) blinded to the clinico-pathological characteristics of patients in two different settings. There was excellent intra- and inter-observer agreement ($\kappa > 0.8$; Cohen's κ and multi-rater κ tests, respectively). The REMARK criteria were followed.

Statistical Analysis

Disease-free survival (DFS) and breast cancer-specific survival (BCSS) were calculated (see supplementary information). Data analysis was performed using SPSS (SPSS, version 17 Chicago, IL). Where appropriate, Pearson's Chi-square, Fisher's exact, Student's *t* and ANOVAs one-way tests were used. Cumulative survival probabilities were estimated using the Kaplan–Meier method, and differences between survival rates were tested for significance using the log-rank test. Multivariate analysis for survival was performed using the Cox hazard model. The proportional hazards assumption was tested using standard log-log plots. HR and 95 % confidence intervals (95 % CI) were estimated for each variable. All

tests were two sided with a 95 % CI, and a p value < 0.05 was considered significant. For multiple comparisons, a stringent p value at 0.01 was considered significant.

Results

Role of ATF-2 in determining the Inhibitory Effects of Tamoxifen in MCF-7 Breast Cancer Cells

To determine whether ATF-2 is important for breast cancer cell growth and response to tamoxifen, ATF-2 levels were reduced in MCF-7 cells using siRNA. Knockdown of ATF-2 was confirmed by immunoblotting ($p = 0.00052$, Figure 1A and supplementary Figure S1A). Loss of ATF-2 did not have a significant effect on cell proliferation, as assessed through cell counting (Figure 1B) and cell cycle distribution analyses by FACS (Figure 1C). However, the loss of ATF-2 significantly attenuated the growth-inhibitory effects of tamoxifen at concentrations as low as 10 nM, whereas re-constitution of ATF-2 reverted the silencing effect similar to the siControl (Figure 1D).

To determine the potential effect of ATF-2 loss on the effects of tamoxifen on anchorage-independent growth of MCF-7 cells, soft agar colony formation assays were performed (Figure 1E). In comparison with the control, the number of colonies produced by siATF-2 cells was significantly increased by 39 % ($p = 0.0004$), whereas the number of colonies produced by siControl was at same level as reagent control cells ($p = 0.36$). This result confirmed our SRB assay and indicated that ATF-2 is key to the effects of tamoxifen in the context of this ER-positive endocrine sensitive cell line.

Effect of Tamoxifen Treatment on Phosphorylation within Activation Domain of ATF-2

Since ATF-2 is required for the growth-inhibitory effects of tamoxifen, and its loss is associated with increased anchorage-independent growth following tamoxifen treatment, the potential influence of tamoxifen on ATF-2 protein levels and phosphorylation status at Thr69/71 was assessed. Total protein levels of ATF-2 were not affected by tamoxifen treatment (Figure 2A, B and S1 B, C), but tamoxifen did enhance ATF-2 phosphorylation in a concentration-dependent manner (Figure 2A and S1 B). Interestingly, tamoxifen induced ATF-2 phosphorylation as early as 5–10 min and was maximal at 45–60 min (Figure 2B and S1 C). Therefore, 1 hour of treatment was used in subsequent experiments.

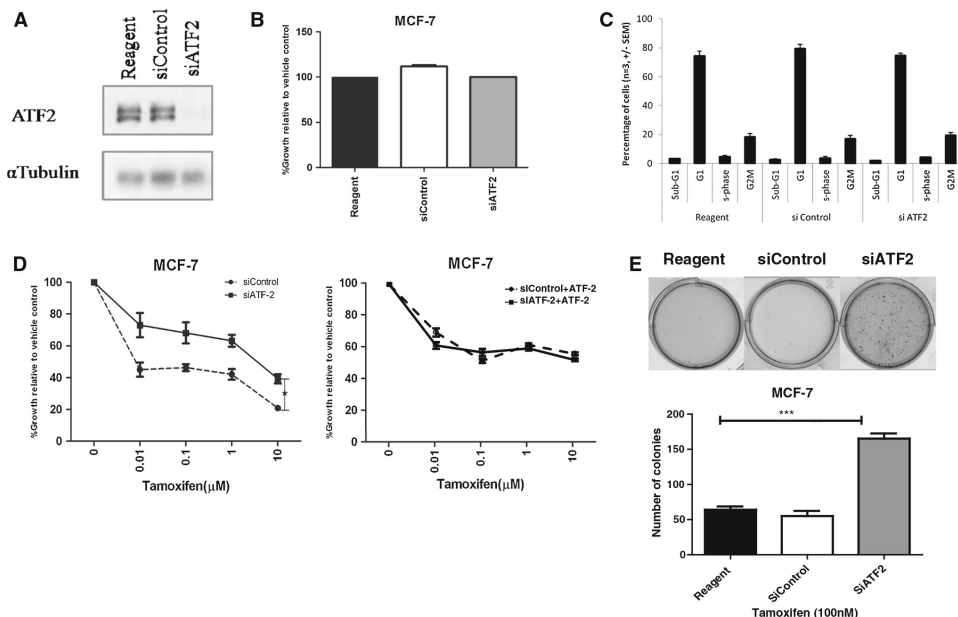


Figure 1. Knockdown of ATF-2 and effects on growth of MCF-7, sensitivity to tamoxifen and modulation of ATF-2 phosphorylation at pATF-2-Thr69/71 by tamoxifen A,B,C.

MCF-7 cells seeded in 96-well plate (B), 60 mm dish (A,C) were treated with either Lipofectamine (Reagent) or transfected with either control or ATF-2 siRNA.

A) Knockdown of ATF-2 was confirmed by immunoblotting for ATF-2 after 72 h of siRNA transfection. α Tubulin was used as loading control, and blots are representative of three independent experiments.

B) For growth assay, basal media were changed on day 3 and stained with SRB on day 3 and 5. Absorbance was calculated relative to reagent control. Error bars represent the standard error of the mean determined from 3 independent experiments.

C) after 48 h of transfection, cells were fixed and then stained with propidium iodide for flow cytometric analysis. The percentage of cells in the sub-G1 (apoptosis), G1, S-phase and G2/M, as determined from 3 independent experiments, is shown. Error bars represent the standard errors of the mean (SEM).

D) dose response curve for tamoxifen in MCF-7 after transfection with control siRNA or siRNA for ATF-2. Media were changed with Vehicle or Tamoxifen on day 3, and absorbance for SRB was taken on day 5. Results are representative of three independent experiments. Difference between the curves was assessed by two-way ANOVA and $p > 0.05$.

E) The growth of siRNA cells was assessed by soft agar assays after 21 days of tamoxifen treatment using Oxford Optronix Gel Count. Results were obtained from three separate assays (mean \pm SE). Statistical analyses were conducted by Student's t-test; *** $p < 0.05$, vs reagent control.

The tamoxifen concentration-dependent increase in ATF-2 phosphorylation was also seen using an antibody that selectively detects phosphorylated Thr71 (supplementary Figure S2). Given that ATF-2 is phosphorylated by p38, ERK1/2 and JNK1/2, we sought to document the effects of tamoxifen on these upstream kinases. Tamoxifen treatment increased phosphorylation levels of p38, JNK1/2 and ERK1/2, while the total protein levels remained unaltered (supplementary Figure S3).

Genomic Locations of pATF-2 in MCF-7 Cells, Proximal Genes and Corresponding Cellular Pathways

Due to the apparent role of ATF-2 in endocrine response, we next aimed to identify which genes could potentially be direct targets of phosphorylated ATF-2. Therefore, we analysed the genome-wide chromatin binding patterns of pATF-2 in MCF-7 cells using ChIP-seq. Proliferating MCF-7 cells were treated with 100nM tamoxifen for 1 h to induce ATF-2 phosphorylation. For immunoprecipitation, antibodies for ATF-2 and pATF-2 (Thr71) were applied, and only peaks were considered that were shared by both antibodies to minimize noise.

Both ATF-2 and pATF-2 gave distinct peaks as exemplified at the NR_047479 promoter (Figure 3A). ChIP-qPCR was performed to validate a number of the binding sites detected by ChIP-seq. (Supplementary Figure S4). Between ATF-2 and pATF-2, 1038 chromatin binding regions were found to be shared, where the strong chromatin binding sites for ATF-2 also provided the most intense pATF-2 signal, as shown in a heatmap visualization where the peaks were ranked according to raw signal intensity (Figure 3B).

Motif analyses indicated ATF-2 binding motifs to be enriched, as expected (Figure 3C). In addition, binding motifs for nuclear transcription factor Y (NFY), nuclear receptor subfamily 1, group 1, member 2 (NR1I2), nuclear receptor subfamily 4, group A, member 1 (NR4A1) and pleiomorphic adenoma gene 1 (PLAG1) were among the top enriched motifs.

pATF-2 was strongly promoter enriched, and gene-proximal binding was mainly found within the first 5 kb from the transcription start site with a strong bias of upstream binding from the transcription start site (Figure 3D). Ingenuity pathway analysis of the 227 genes with proximal pATF-2 binding (Supplementary Table S1) illustrated pathways enriched for cellular assembly and signalling (pathway 1, 3, 7), development and cancer (pathway 2, 4, 5, 8, 9, 10) as well as cell death and survival (pathway 6) (Figure 3E).

Utilising the entire geneset with proximal pATF-2 binding, we examined their potential association with distant metastasis-free survival in a

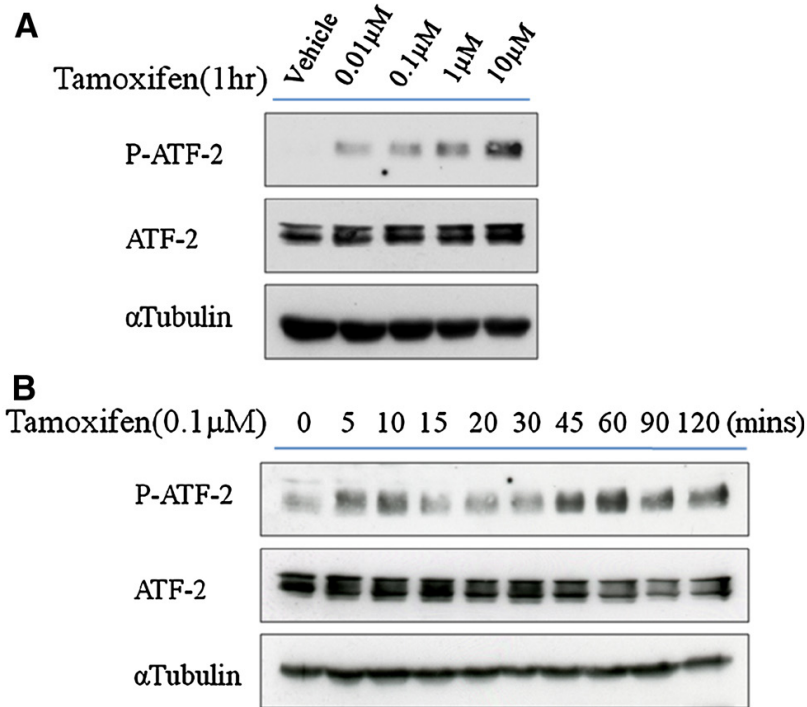


Figure 2. Modulation of ATF-2 phosphorylation at pATF-2-Thr69/71 by tamoxifen A-B. Exponentially growing MCF-7 cells in their basal media were treated with increasing concentrations of tamoxifen for 1 h (**A**) or with ethanol (vehicle) or 0.1 μ M tamoxifen for indicated times (**B**). Cells were harvested for immunoblotting and probed with indicated antibodies. Tubulin was used as loading control. Results are representative of three independent experiments.

publically available cohort of 249 breast cancer patients who received adjuvant tamoxifen treatment³². Patients were classified using unsupervised hierarchical clustering, which revealed two distinct clusters of patients (Figure 4A). Distant metastasis-free survival is significantly different between these two groups of patients (HR = 3.05, CI 1.86–5, $p = 3e-6$; Figure 4B). In contrast, no association to survival was found in a cohort of 209 ER-positive breast cancer patients who did not receive any adjuvant endocrine treatment³³ (HR = 0.92, CI 0.59–1.44, $p = 0.712$; Figure 3C–D).

Expression of ATF-2 mRNA in Primary and Secondary Breast Cancer Samples

ATF-2 mRNA levels were determined in pooled normal breast tissue ($n = 5$) and compared to primary breast cancer ($n = 20$) and metastatic breast cancer samples ($n = 20$). As compared to normal breast tissue, ATF-2

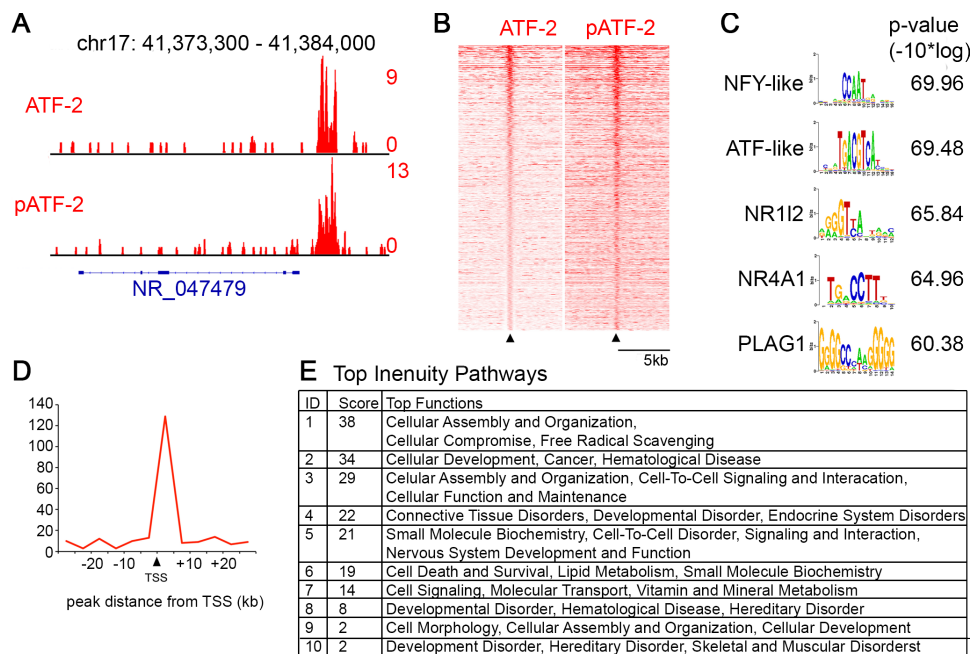


Figure 3. pATF-2-Thr71 genome-wide chromatin binding patterns indicate distinct gene signature. **A)** genome browser snapshot illustrating chromatin binding sites for ATF-2 and pATF-2 at the NR_047479 promoter. Tag count and genomic coordinates are indicated. **B)** heatmap visualization of the ranked shared peaks of ATF-2 and pATF-2. Arrowhead indicated top of the peak. Scale bar shows 5 kb. **C)** top enriched motifs for the shared chromatin binding events of ATF-2 and pATF-2. p-values are indicated. **D)** graph showing the distribution of pATF-2 peaks related to the most proximal gene. **E)** ingenuity pathway analysis of the 227 genes with a proximal pATF-2 chromatin binding event.

was significantly lower in primary breast cancers ($p = <0.05$). While the secondary deposits like the primary deposits had significantly less ATF-2 than normal controls, there was no significant difference seen between the primary and secondary breast cancer deposits with regard to ATF-2 expression (Supplementary Figure S5).

ATF-2 and pATF-2 Expression in Human Breast Cancer and Correlation with Clinico-pathological Features and Outcome

To explore the expression and relevance of ATF-2 and pATF-2 in human breast cancer, IHC was performed on a previously validated TMA of 1,650 breast cancers^{34,35}. Correlations were made with DFS or BCSS, for clinic-pathological parameters see supplementary Table S2. As is to be expected from a transcriptional regulator, IHC revealed that ATF-2 and pATF-2-Thr71 had a nuclear location (Supplementary Figure S6A and B).

689/1388 (49.6 %) and 680/1516 (44.9 %) of breast cancers showed low or no expression of ATF-2 and its phosphorylated active form pATF-2-pThr71. Low expression of both ATF-2 and pATF-2-pThr71 was significantly associated with aggressive and adverse pathological features including high grade, glandular de-differentiation, high mitotic index, high proliferation rate, high pleomorphism, and invasive ductal no special type (IDC-NST) (p values < 0.0001 ; Table 1). Low expression of both ATF-2 and its active form pATF-2-pT71 were also associated with negative expression of hormone receptors including ER α , progesterone receptor (PR) and the androgen receptor (AR) (p values < 0.0001 ; Table 1), with both ATF-2 and pATF-2-pT71 being inversely related to the triple negative and basal-like phenotypes (Table 1). In addition, low ATF-2 and pATF-2-pThr71 expression was significantly associated with low expression of DNA repair proteins such as BRCA1, XRCC1, ATM and TOP2A ($p < 0.0001$), and other tumour suppressor proteins such as p53, p16 and FHIT ($p < 0.0001$), reflecting a higher level of genomic instability.

Notably, low ATF-2/pATF-2-pThr71 expression was also significantly associated with low expression of both cell cycle and apoptosis regulatory proteins such as p21, MDM4, p27, Bcl2 and Bax. Moreover, high expression of epithelial-mesenchymal transition (EMT) proteins such as vimentin, smooth muscle actin (SMA), p63, cytokeratin (CK) 5/6 and p-cadherin was more common in samples with low expression of either ATF-2 and/or pATF-2-pThr71 (Table 1). Furthermore, pATF-2-pThr71 was significantly associated with both p-p38 and pJNK1/2, which are both known to phosphorylate ATF-2 at Thr71.

Expression of ATF-2 was neither associated with DFS or BCSS in the whole cohort (Supplementary Figure S7A) nor in the ER-positive cases (Supplementary Figure S7B). Furthermore, no difference in outcome based on ATF-2 expression was seen in patients treated with or without tamoxifen (Supplementary Figure S7C–E). By contrast, high pATF-2-pThr71 was associated with a significantly longer DFS and BCSS in the whole cohort as well as in the ER-positive cases (Figure 5A, B). Moreover, high expression of pATF-2-pThr71 was associated with significantly longer DFS (HR: 0.66, 95 % CI: 0.51–0.86, $p = 0.002$) and BCSS (HR: 0.69, 95 % CI: 0.51–0.92, $p = 0.01$) in patients exposed to tamoxifen (Figure 5E). No difference in DFS or BCSS was observed in ER α -positive patients who did not receive tamoxifen (Figure 5C, D).

A test for interaction confirms that pATF-2-pT71 is both a prognostic and predictive factor for response to tamoxifen in ER α -positive/high risk (NPI > 3.4) patients (supplementary Table S3). Furthermore, multivariate analysis confirmed pATF-2-pThr71 as associated with decreased recurrence (HR = 0.78, CI 95 %: 0.61–0.98) and death (HR = 0.78, CI 95 %: 0.64–0.95) from breast cancer (Table 2).

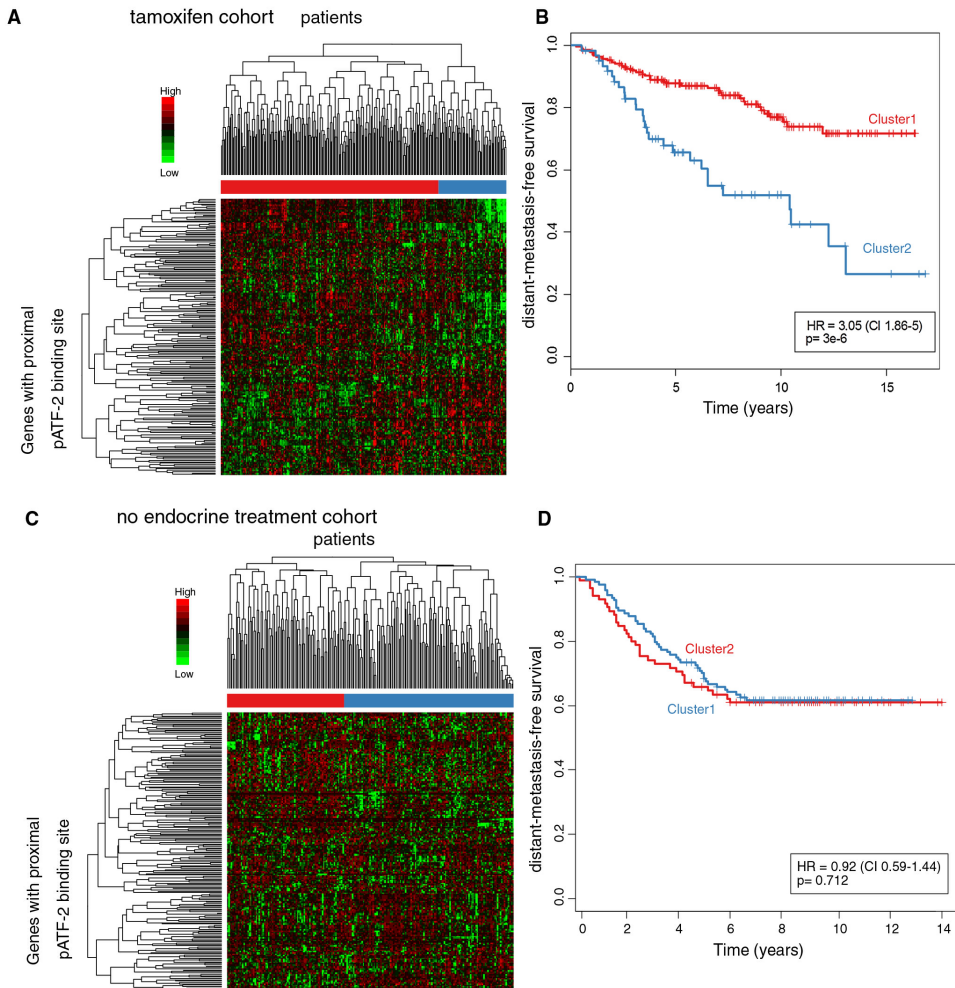


Figure 4. Genes with a proximal pATF-2 binding sites provide a signature for time to distant metastasis. **A/C.** Heatmap, depicting genes with a proximal pATF-2 chromatin binding site (rows) in a cohort of 249 breast cancer patients (columns) who received adjuvant tamoxifen treatment (**A**) or did not receive any endocrine treatment (**C**). Unsupervised hierarchical clustering identified two patient subgroups based on differential gene expression. **B/D.** Kaplan–Meier survival curves, depicting distant metastasis-free survival for the patients in **A** and **C** using the two different subgroups of patients identified through differential expression of genes with proximal pATF-2 binding.

Table 1. Clinico-pathological characteristics and tumour biomarkers and correlation with ATF-2 and pATF-2-pThr71

Variables	ATF2		p value	pATF2		p value
	Low (n = 689)	High (n = 699)		Low (n = 680)	High (n = 836)	
Pathological parameters						
Tumour size			0.229			0.125
T1 a + b (= <1.0)	63 (9)	69 (9.9)		63 (9.3)	89 (10.7)	
T1 c (> 1.0–2.0)	348 (49.9)	364 (52.2)		322 (47.7)	434 (52.2)	
T2 (> 2.0–5.0)	263 (37.7)	252 (36.2)		273 (40.4)	287 (34.5)	
T3 (>5)	23 (3.3)	12 (1.7)		17 (2.5)	22 (2.6)	
Lymph node stage			0.026			0.397
Negative	447 (64)	406 (58.1)		408 (60.4)	523 (62.7)	
Positive (1–3 nodes)	200 (28.7)	218 (31.2)		201 (29.7)	244 (29.3)	
Positive (>3 nodes)	51 (7.3)	75 (10.7)		67 (9.9)	67 (8.0)	
Tumour grade			<0.0001			<0.0001
G1	117 (16.8)	122 (17.5)		101 (15.0)	152 (18.3)	
G2	177 (25.4)	288 (41.3)		174 (25.8)	331 (39.8)	
G3	403 (57.8)	287 (41.2)		400 (59.3)	349 (41.9)	
Mitotic index			<0.0001			<0.0001
M1 (low; mitoses < 10)	217 (31.5)	285 (40.9)		192 (28.6)	351 (42.4)	
M2 (medium; mitoses 10–18)	107 (15.5)	150 (21.6)		112 (16.7)	264 (19.8)	
M3 (high; mitoses > 18)	365 (53)	261 (37.5)		367 (54.7)	312 (37.7)	
Pleomorphism			<0.0001			<0.0001
P1	18 (2.6)	21 (3.0)		17 (2.5)	25 (3.0)	
P2	234 (34.1)	312 (44.8)		210 (31.3)	375 (45.5)	
P3	435 (63.3)	363 (52.2)		444 (66.2)	425 (51.5)	
Tubule formation			<0.0001			<0.0001
T1	38 (5.5)	36 (5.2)		25 (3.7)	55 (6.7)	
T2	198 (28.7)	261 (37.5)		215 (32.0)	277 (33.5)	
T3	453 (65.7)	399 (57.3)		431 (64.2)	495 (59.9)	
Tumour type			<0.0001			<0.0001
IDC-NST	376 (62.3)	339 (54.8)		372 (62.6)	395 (55.6)	
Medullary/atypical	22 (3.6)	5 (0.8)		22 (3.7)	7 (1.0)	
Tubular carcinoma	103 (17.1)	143 (23.1)		99 (16.7)	161 (22.6)	

Variables	ATF2		p value	pATF2		p value
	Low (n = 689)	High (n = 699)		Low (n = 680)	High (n = 836)	
Invasive lobular carcinoma	51 (8.4)	76 (12.3)		52 (8.8)	87 (12.2)	
Others	52 (8.6)	56 (9.0)		49 (8.2)	61 (8.6)	
Lymphovascular invasion			0.703			0.184
Yes	465 (67.2)	473 (68.2)		447 (66.3)	573 (69.5)	
No	227 (32.8)	221 (31.8)		227 (33.7)	251 (30.5)	
Pc-JUN			<0.0001			<0.0001
Negative	351 (55.4)	225 (35.6)		411 (66.9)	199 (26.5)	
Positive	283 (44.6)	407 (64.4)		203 (33.1)	551 (73.5)	
P-JNK			<0.0001			<0.0001
Negative	495 (76.9)	414 (992.6)		479 (84.2)	424 (58.9)	
Positive	149 (23.1)	247 (37.4)		90 (15.8)	296 (41.1)	
p-p38			<0.0001			<0.0001
Negative	484 (89.6)	449 (78.1)		498 (93.8)	470 (75.4)	
Positive	56 (10.4)	126 (21.9)		33 (6.2)	153 (24.6)	
SRC3			<0.0001			<0.0001
Negative	418 (66.9)	282 (43.8)		153 (25.2)	52 (6.8)	
Positive	207 (33.1)	362 (56.2)		453 (74.8)	713 (93.2)	
Oestrogen receptor			<0.0001			<0.0001
Negative	244 (35.6)	107 (15.6)		205 (30.8)	181 (22.0)	
Positive	442 (64.4)	580 (84.4)		461 (69.2)	640 (78.0)	
Progesterone receptor			<0.0001			<0.0001
Negative	320 (49.0)	212 (32.7)		301 (47.6)	288 (37.0)	
Positive	333 (51.0)	437 (67.3)		331 (52.4)	490 (63.0)	
Androgen receptor			<0.0001			<0.0001
Negative	271 (49.1)	141 (25.0)		261 (47.5)	170 (26.5)	
Positive	281 (50.9)	422 (75.0)		288 (52.5)	471 (73.5)	
EGFR			0.006			0.533
Negative	422 (77.6)	473 (84.0)		429 (79.7)	522 (81.2)	
Overexpression	122 (22.4)	90 (16.0)		109 (20.3)	121 (18.8)	
HER2			0.977			0.786
Negative	616 (89.1)	613 (89.1)		591 (88.6)	732 (89.1)	
Overexpression	75 (10.9)	75 (10.9)		76 (11.4)	90 (10.9)	
HER3			0.812			0.656
Negative	286 (50.4)	276 (49.7)		271 (50.1)	326 (48.8)	

Variables	ATF2		p value	pATF2		p value
	Low (n = 689)	High (n = 699)		Low (n = 680)	High (n = 836)	
Overexpression	281 (49.6)	279 (50.3)		270 (49.9)	342 (51.2)	
HER4			0.018			0.365
Negative	221 (39.3)	259 (46.3)		224 (41.3)	299 (43.9)	
Overexpression	342 (60.7)	301 (53.8)		318 (58.7)	382 (56.1)	
P53			<0.0001			<0.0001
Negative	421 (74.5)	483 (84.7)		414 (74.5)	554 (83.8)	
Positive	144 (25.5)	87 (15.3)		142 (25.5)	107 (16.2)	
Ki67			0.006			0.003
Negative	192 (33.0)	239 (40.8)		178 (32.2)	288 (40.4)	
Positive	390 (67.0)	347 (59.2)		375 (67.8)	424 (59.6)	
BRCA1			<0.0001			<0.0001
Negative	129 (26.6)	59 (11.6)		115 (24.0)	87 (14.9)	
Positive	356 (73.4)	451 (88.4)		365 (76)	495 (85.1)	
CK18			<0.0001			0.002
Negative	86 (15.7)	26 (4.6)		73 (13.4)	50 (7.8)	
Positive	461 (84.3)	536 (95.4)		471 (86.6)	590 (92.2)	
CK5/6			<0.0001			0.103
Negative	463 (78.5)	532 (88.7)		480 (81.8)	580 (85.2)	
Positive	127 (21.5)	68 (11.3)		107 (18.2)	101 (14.8)	
CK14			0.315			0.239
Negative	506 (86.6)	527 (88.6)		505 (86.8)	603 (88.9)	
Positive	78 (13.4)	68 (11.4)		77 (13.2)	75 (11.1)	
E-cadherin			0.186			0.259
Negative	41 (7.1)	31 (5.3)		40 (7.0)	37 (5.5)	
Positive	534 (92.9)	558 (94.7)		529 (93)	638 (94.5)	
Triple negative phenotype			<0.0001			<0.0001
No	491 (72.5)	628 (91.8)		508 (77.1)	698 (85.5)	
Yes	186 (27.5)	56 (8.2)		151 (22.9)	118 (14.5)	
Basal like phenotype			<0.0001			<0.0001
No	537 (81.2)	644 (95.3)		548 (84.4)	725 (91.3)	
Yes	124 (18.8)	32 (4.7)		101 (15.6)	69 (8.7)	

Discussion

In the present study, we have investigated the potential role of ATF-2 and its phosphorylation within the AD in mediating the actions of tamoxifen in the luminal breast cancer cell line MCF-7, including determining the genomic locations of ATF-2 when phosphorylated by tamoxifen within the AD. Furthermore, the expression of ATF-2 in healthy breast tissue and paired primary and secondary human breast cancer samples, as well in a large, well-characterised human breast cancer series were defined, and its influence on outcome was both with and without adjuvant tamoxifen treatment. We found that ATF-2 expression is decreased in primary breast tumours as compared to healthy tissue, in line with a previous report²⁸ supporting the view that ATF-2 is a tumour suppressor in breast cancer.

We have, for the first time, shown that the expression of ATF-2 in paired primary and secondary breast cancer is similar, suggesting that alterations in ATF-2 levels are not involved in the metastatic process. This however, does not exclude the possibility that post-translational modification or mutations of ATF-2 may be important in metastasis formation. Interestingly, *in vitro* data in breast cancer would suggest the involvement of ATF-2 in the promotion of tumourigenesis^{23,24}. This apparent dual function of ATF-2 is also observed in skin tumourigenesis where ATF-2 has both oncogenic and tumour-suppressive activities^{38,39}.

Proliferation of MCF-7 cells was not influenced by the loss of ATF-2, and no effects were seen on the cell cycle. These data are in keeping observations of mouse embryonic fibroblasts (MEFs) where no effect of ATF-2 knockout was seen, either on growth or the cell cycle²⁸. However, the loss of ATF-2 leads to a loss in the growth-inhibitory effects of tamoxifen, indicating that ATF-2 is the key to the effects of tamoxifen in the context of this ER-positive endocrine sensitive cell line. ATF-2 is known to be critical in stress-induced apoptosis, as well as in hypoxia- and anisomycin-induced apoptosis, with MEFs that lack ATF-2 being resistant to such treatment^{18,28}.

Utilising the large and well-characterised Nottingham Tenovus Primary breast cancer, we have shown that ATF-2 and its phosphorylation within the AD (pATF-2-Tyr71) are significantly associated with a luminal A phenotype, while its absence is strongly associated with a basal phenotype. In a significantly smaller series of 133 breast cancers, pATF-2 (Thr69/71), detected by Western blotting, was associated with ER positivity and low grade tumours, while positivity (Thr69) by IHC was associated with low clinical stage²⁹. However, the correlations seen with Western blotting were not seen by IHC and vice versa³⁰. Furthermore, in this previous report, high expression of ATF-2 by Western blotting was associated with a significantly shorter overall survival, while phosphorylation of ATF-2-Thr69 by IHC was associated with a better overall survival³⁰; however, no

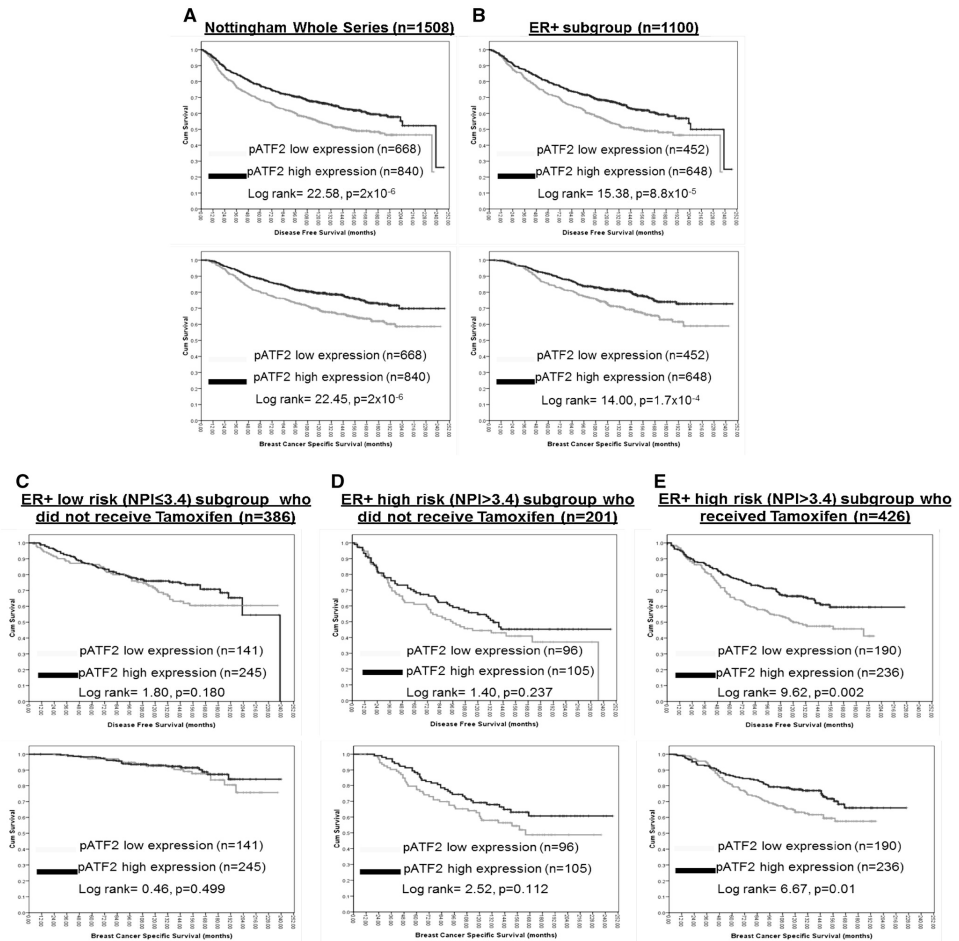


Figure 5. Kaplan–Meier survival curve pATF-2-Thr71 Kaplan-Meier survival curve showing percentage disease-free survival (DFS) and breast cancer-specific survival (BCCS) with and without tamoxifen of patients with pATF-2-overexpressing tumours compared with all other patients:

- A)** entire Nottingham cohort.
- B)** ER α -positive Cohort.
- C)** ER α -positive patients NPI < 3.4 who did not receive tamoxifen.
- D)** ER α -positive patients NPI > 3.4 who did not receive tamoxifen.
- E)** ER α -positive patients NPI > 3.4 who received tamoxifen.

information was presented regarding the treatment of these cases and the possible influence of ATF-2 or pATF-2 on treatment related outcome. The data from our current study, of a well-defined larger series and using a wider range of known prognostic markers, show that pATF-2 is associated with positive prognostic factors, consistent with an initial smaller study, albeit by a different methodology³⁰.

We found no difference in outcome based on expression of ATF-2; however, expression of pATF-2-Thr71 was significantly associated with DFS and BCSS in the whole cohort as well as those patients who were ER positive. Furthermore, multivariate analysis confirmed that pATF-2-pThr71 was associated with both a decreased risk of recurrence and death from breast cancer. With regard to treatment, improvement in DFS and BCSS was only seen in those patients with pATF-2-pThr71 who received tamoxifen, with a test for interaction confirming that pATF-2-pT71 is both a prognostic and predictive factor for response to tamoxifen.

Our results raised the question: what are the molecular mechanisms that underlie the role of ATF-2 in response to tamoxifen treatment? The ChIP-seq for pATF-2-Tyr71 identified, aside from ATF-2 motif analyses, enrichment for a number of other transcription factors that may play a role. ATF-2 is known to affect transcription of target genes in trans through its interaction with other transcription factors⁴⁰. Phosphorylated ATF-2 is clearly enriched in promoter regions upstream of responsive genes, since we generated a comprehensive list of 227 genes with such a proximal pATF-2 binding site. These genes were enriched for functions associated with oncogenic (cell proliferation and cell death) and metastatic (cell-to-cell signalling, connective tissue disorders) processes. The enrichment for pathways involved in development is consistent with the known role of ATF-2 in neurological and skeletal development⁴¹. The currently known transcriptional targets of ATF-2 by functional groups, specific stimuli and cell types have recently been documented³⁹⁻⁴², and these are consistent with the enriched pathways reported here.

Using the proximal pATF-2-binding sites unsupervised hierarchical clustering was undertaken in two publically available cohorts of breast cancer patients treated with and without endocrine therapy^{33,34}, this revealed that only in those patients who were treated with tamoxifen was there a significant difference in outcome. While motif analyses of the proximal binding sites indicated that in addition to the expected enrichment of ATF, other enriched motifs included NFY, NR1I2 and NR4A1. These motifs are of interest given that phosphorylated ATF-2 interacts with NFY, regulating c-JUN expression in gonadotropes⁴³, while NR4A1 and ATF-2 have been shown to have a synergistic effect on aldosterone synthase/CYP11B2 promoter activity⁴⁴. Synergism and protein-protein interactions of NR4A1 and ATF/CREB members have also been described in the transcription of the proopiomelanocortin gene⁴⁵. While the CREB/ATF family CREB has been shown to directly interact with NR1I2 leading to repression of glucose-6-phosphatase⁴⁶.

The current study shows that tamoxifen treatment did not affect overall levels of ATF-2; it caused a dose-dependent phosphorylation of ATF-2 within the AD, at physiologically relevant concentrations.

Table 2. Multivariate analysis using Cox regression analysis confirms that pATF-2-Thr71 protein expression is independent prognostic factor for both Disease-Free Survival (DFS) and Breast Cancer-Specific Survival (BCSS)

Variable	BCSS at 10 years		DFS at 10 years	
	HR (CI 95 %)	<i>p</i>	HR (CI 95 %)	<i>p</i>
ATF2-T71(high expression)	0.77 (0.61–0.98)	0.034**	0.78 (0.64–0.95)	0.013**
Tumour size	1.07 (0.95–1.19)	0.265	1.09 (1.00–1.18)	0.063
Grade*				
G1	1.00	0.034**	1.00	0.971
G2	1.32 (0.77–2.28)		1.03 (0.73–1.44)	
G3	1.87 (1.06–3.30)		1.05 (0.72–1.53)	
Lymph node stage				
Negative	1.00	2.2×10^{-13} **	1.00	3.5×10^{-15} **
Positive (1–3 nodes)	1.62 (1.22–2.14)		1.34 (1.06–1.68)	
Positive (>3 nodes)	3.85 (2.72–5.44)		3.56 (2.62–4.84)	
Endocrine therapy (no)	1.14(0.89–1.47)	0.311	0.95 (0.77–1.18)	0.632
Chemotherapy (no)	1.26 (0.93–1.72)	0.141	1.30 (1.01–1.68)	0.042**
Bcl2 expression (positive)	0.46 (0.35–0.61)	2.1×10^{-8} **	0.54 (0.43–0.68)	7.2×10^{-8} **
Ki67 expression (high)	1.77 (1.16–2.51)	0.001**	1.30 (1.01–1.66)	0.042**
ER expression (negative)	1.95 (1.35–2.81)	3.9×10^{-4} **	1.62(1.17–2.25)	0.004**
HER2 (overexpression)	1.41 (1.02–1.96)	0.039**	1.21 (0.90–1.64)	0.206
PR expression (negative)	0.62 (0.45–0.86)	0.004**	0.78 (0.60–1.02)	0.068

Phosphorylation of ATF-2 within the AD is required to de-repress ATF-2 and results in transcriptional activity¹⁴; phosphorylation within the AD at Thr69 and/or Thr71 being mediated by c-Jun N-terminal protein kinase (JNK) and p38^{14,15,18}. Previously, tamoxifen has been shown to activate p38⁴⁷ and JNK⁴⁸ with attenuation of these pathways leading to a loss in tamoxifen-induced apoptosis. Tamoxifen has also been shown to induce the phosphorylation of ATF-2 at Tyr71 via p38⁴⁹. In the current study, we demonstrate that tamoxifen can lead to phosphorylation of p38, JNK and MAPK simultaneously. Therefore, tamoxifen may be able to augment ATF-2 phosphorylation within the AD via these kinases and so enhancing its transcriptional activity. Alternatively, it may cause the phosphorylation of other AP-1 family members such as c-JUN, which in conjunction with pATF-2 results in the transcriptional events leading to the outcomes observed.

In light of the tamoxifen-induced phosphorylation of ATF-2 reported here, and given that phosphorylation of ATF-2 within the AD is required for transcriptional activation^{14,15}, this would indicate that transcriptional

events induced by tamoxifen via pATF-2-Tyr71 are key to the observed benefit in the clinical cohort of patients. The lack of benefit in those not treated with tamoxifen suggests that the transcriptional events in the presence of basal pATF-2-Tyr71 alone are not sufficient. While the significant association between the presence of both p-JNK and p-p38, and pATF-2-Tyr71 in human breast cancers, and the poorer outcome observed in patients with low pATF-2-Tyr71 who were given tamoxifen would support the hypothesis that a functional JNK and/or p38 pathways are required for tamoxifen-induced phosphorylation within the AD. Of note, inactivating mutations in the JNK signalling pathway are one of the most distinct genomic features of luminal breast cancers⁵⁰, with activation of AKT via activating PI3 kinase mutations providing a further route for this pathway to be abrogated in luminal breast cancers⁵⁰. Therefore, dysfunctionality within the JNK pathway may influence response to tamoxifen.

In summary, we provide evidence for a role of ATF-2 in determining sensitivity to tamoxifen treatment in ER-positive breast cancer as demonstrated by (1) loss of ATF-2 abrogating the growth-inhibitory effects of tamoxifen, (2) treatment with tamoxifen resulting in phosphorylation of ATF-2 in the known activation domain, (3) identification of p-ATF-2-Tyr71 responsive genes and (4) improved disease-free and overall survival in high risk ER-positive breast cancers treated with tamoxifen. Future studies will be required to investigate whether pATF-2 measurement could assist clinicians to predict which patients would benefit from tamoxifen treatment. Furthermore, the potential importance of functionality within the JNK pathway on phosphorylation of ATF-2 within the AD and its potential influence on response to tamoxifen treatment require further investigation.

Acknowledgments

Carlo Palmieri was supported by a clinician scientist fellowship from Cancer Research UK, Wilbert Zwart by a KWF Dutch Cancer Society Fellowship and a VENI scholarship from the Dutch Organisation for Scientific Research NWO, and Jason Carroll by an ERC starting grant and an EMBO Young investigator award. We thank Angie Gillies (University of Leicester) for technical help with immunohistochemistry. We would also like to acknowledge the support of Cancer Research UK Cambridge Research Institute, The Netherlands Cancer Institute and A Sisters Hope. The Department of Molecular and Clinical Cancer Medicine forms part of the North West Cancer Centre-University of Liverpool which is funded by North West Cancer Research. Research support is also received from The Clatterbridge Cancer Charity.

References

- 1 Goldhirsch, A. *et al.* Meeting highlights: international expert consensus on the primary therapy of early breast cancer 2005. *Annals of oncology: official journal of the European Society for Medical Oncology / ESMO* **16**, 1569-1583, (2005).
- 2 Early Breast Cancer Trialists' Collaborative, G. *et al.* Relevance of breast cancer hormone receptors and other factors to the efficacy of adjuvant tamoxifen: patient-level meta-analysis of randomised trials. *Lancet* **378**, 771-784, (2011).
- 3 Ali, S. & Coombes, R. C. Endocrine-responsive breast cancer and strategies for combating resistance. *Nature reviews. Cancer* **2**, 101-112, (2002).
- 4 Palmieri, C., Patten, D. K., Januszewski, A., Zucchini, G. & Howell, S. J. Breast cancer: current and future endocrine therapies. *Molecular and cellular endocrinology* **382**, 695-723, (2014).
- 5 Hai, T. & Hartman, M. G. The molecular biology and nomenclature of the activating transcription factor/cAMP responsive element binding family of transcription factors: activating transcription factor proteins and homeostasis. *Gene* **273**, 1-11, (2001).
- 6 Hai, T. W., Liu, F., Coukos, W. J. & Green, M. R. Transcription factor ATF cDNA clones: an extensive family of leucine zipper proteins able to selectively form DNA-binding heterodimers. *Genes & development* **3**, 2083-2090, (1989).
- 7 Hai, T. & Curran, T. Cross-family dimerization of transcription factors Fos/Jun and ATF/CREB alters DNA binding specificity. *Proceedings of the National Academy of Sciences of the United States of America* **88**, 3720-3724, (1991).
- 8 Matsuda, S., Maekawa, T. & Ishii, S. Identification of the functional domains of the transcriptional regulator CRE-BP1. *The Journal of biological chemistry* **266**, 18188-18193, (1991).
- 9 van Dam, H. *et al.* Heterodimer formation of cJun and ATF-2 is responsible for induction of c-jun by the 243 amino acid adenovirus E1A protein. *The EMBO journal* **12**, 479-487, (1993).
- 10 Kim, H. S., Choi, E. S., Shin, J. A., Jang, Y. K. & Park, S. D. Regulation of Swi6/HP1-dependent heterochromatin assembly by cooperation of components of the mitogen-activated protein kinase pathway and a histone deacetylase Clr6. *The Journal of biological chemistry* **279**, 42850-42859, (2004).
- 11 Agelopoulos, M. & Thanos, D. Epigenetic determination of a cell-specific gene expression program by ATF-2 and the histone variant macroH2A. *The EMBO journal* **25**, 4843-4853, (2006).
- 12 Bruhat, A. *et al.* ATF2 is required for amino acid-regulated transcription by orchestrating specific histone acetylation. *Nucleic acids research* **35**, 1312-1321, (2007).
- 13 Li, X. Y. & Green, M. R. Intramolecular inhibition of activating transcription factor-2 function by its DNA-binding domain. *Genes & development* **10**, 517-527, (1996).

- 14 Gupta, S., Campbell, D., Derijard, B. & Davis, R. J. Transcription factor ATF2 regulation by the JNK signal transduction pathway. *Science* **267**, 389-393, (1995).
- 15 Livingstone, C., Patel, G. & Jones, N. ATF-2 contains a phosphorylation-dependent transcriptional activation domain. *The EMBO journal* **14**, 1785-1797, (1995).
- 16 Raugeaud, J., Whitmarsh, A. J., Barrett, T., Derijard, B. & Davis, R. J. MKK3- and MKK6-regulated gene expression is mediated by the p38 mitogen-activated protein kinase signal transduction pathway. *Molecular and cellular biology* **16**, 1247-1255, (1996).
- 17 Ouwens, D. M. *et al.* Growth factors can activate ATF2 via a two-step mechanism: phosphorylation of Thr71 through the Ras-MEK-ERK pathway and of Thr69 through RalGDS-Src-p38. *The EMBO journal* **21**, 3782-3793, (2002).
- 18 van Dam, H. *et al.* ATF-2 is preferentially activated by stress-activated protein kinases to mediate c-jun induction in response to genotoxic agents. *The EMBO journal* **14**, 1798-1811, (1995).
- 19 Tsay, Y. G., Wang, Y. H., Chiu, C. M., Shen, B. J. & Lee, S. C. A strategy for identification and quantitation of phosphopeptides by liquid chromatography/tandem mass spectrometry. *Analytical biochemistry* **287**, 55-64, (2000).
- 20 Sakurai, A., Maekawa, T., Sudo, T., Ishii, S. & Kishimoto, A. Phosphorylation of cAMP response element-binding protein, CRE-BP1, by cAMP-dependent protein kinase and protein kinase C. *Biochemical and biophysical research communications* **181**, 629-635, (1991).
- 21 Yamasaki, T., Takahashi, A., Pan, J., Yamaguchi, N. & Yokoyama, K. K. Phosphorylation of Activation Transcription Factor-2 at Serine 121 by Protein Kinase C Controls c-Jun-mediated Activation of Transcription. *The Journal of biological chemistry* **284**, 8567-8581, (2009).
- 22 Bhoumik, A. *et al.* ATM-dependent phosphorylation of ATF2 is required for the DNA damage response. *Molecular cell* **18**, 577-587, (2005).
- 23 Lewis, J. S. *et al.* Activation of cyclin D1 by estradiol and spermine in MCF-7 breast cancer cells: a mechanism involving the p38 MAP kinase and phosphorylation of ATF-2. *Oncology research* **15**, 113-128, (2005).
- 24 Song, H., Ki, S. H., Kim, S. G. & Moon, A. Activating transcription factor 2 mediates matrix metalloproteinase-2 transcriptional activation induced by p38 in breast epithelial cells. *Cancer research* **66**, 10487-10496, (2006).
- 25 Lewis, J. S. *et al.* Differential effects of 16alpha-hydroxyestrone and 2-methoxyestradiol on cyclin D1 involving the transcription factor ATF-2 in MCF-7 breast cancer cells. *Journal of molecular endocrinology* **34**, 91-105, (2005).
- 26 Hayakawa, J., Depatie, C., Ohmichi, M. & Mercola, D. The activation of c-Jun NH2-terminal kinase (JNK) by DNA-damaging agents serves to promote drug resistance via activating transcription factor 2 (ATF2)-dependent enhanced DNA repair. *The Journal of biological chemistry* **278**, 20582-20592, (2003).

- 27 Hayakawa, J. *et al.* Identification of promoters bound by c-Jun/ATF2 during rapid large-scale gene activation following genotoxic stress. *Molecular cell* **16**, 521-535, (2004).
- 28 Maekawa, T. *et al.* Reduced levels of ATF-2 predispose mice to mammary tumors. *Molecular and cellular biology* **27**, 1730-1744, (2007).
- 29 Liu, Y., Wang, Y., Li, W., Zheng, P. & Liu, Y. Activating transcription factor 2 and c-Jun-mediated induction of FoxP3 for experimental therapy of mammary tumor in the mouse. *Cancer research* **69**, 5954-5960, (2009).
- 30 Knippen, S. *et al.* Expression and prognostic value of activating transcription factor 2 (ATF2) and its phosphorylated form in mammary carcinomas. *Anticancer research* **29**, 183-189, (2009).
- 31 Lopez-Garcia, J. *et al.* ZNF366 is an estrogen receptor corepressor that acts through CtBP and histone deacetylases. *Nucleic acids research* **34**, 6126-6136, (2006).
- 32 He, H. H. *et al.* Nucleosome dynamics define transcriptional enhancers. *Nature genetics* **42**, 343-347, (2010).
- 33 Loi, S. *et al.* Definition of clinically distinct molecular subtypes in estrogen receptor-positive breast carcinomas through genomic grade. *Journal of clinical oncology : official journal of the American Society of Clinical Oncology* **25**, 1239-1246, (2007).
- 34 Wang, Y. *et al.* Gene-expression profiles to predict distant metastasis of lymph-node-negative primary breast cancer. *Lancet* **365**, 671-679, (2005).
- 35 Ellis, I. O. *et al.* Pathological prognostic factors in breast cancer. II. Histological type. Relationship with survival in a large study with long-term follow-up. *Histopathology* **20**, 479-489, (1992).
- 36 Abdel-Fatah, T. M. *et al.* Bcl2 is an independent prognostic marker of triple negative breast cancer (TNBC) and predicts response to anthracycline combination (ATC) chemotherapy (CT) in adjuvant and neoadjuvant settings. *Annals of oncology : official journal of the European Society for Medical Oncology / ESMO* **24**, 2801-2807, (2013).
- 37 Sultana, R. *et al.* Targeting XRCC1 deficiency in breast cancer for personalized therapy. *Cancer research* **73**, 1621-1634, (2013).
- 38 Berger, A. J. *et al.* Subcellular localization of activating transcription factor 2 in melanoma specimens predicts patient survival. *Cancer research* **63**, 8103-8107, (2003).
- 39 Bhoumik, A. *et al.* Suppressor role of activating transcription factor 2 (ATF2) in skin cancer. *Proceedings of the National Academy of Sciences of the United States of America* **105**, 1674-1679, (2008).
- 40 Choi, J. H., Cho, H. K., Choi, Y. H. & Cheong, J. Activating transcription factor 2 increases transactivation and protein stability of hypoxia-inducible factor 1alpha in hepatocytes. *The Biochemical journal* **424**, 285-296, (2009).
- 41 Reimold, A. M. *et al.* Chondrodysplasia and neurological abnormalities in ATF-2-deficient mice. *Nature* **379**, 262-265, (1996).
- 42 Lau, E. & Ronai, Z. A. ATF2 - at the crossroad of nuclear and cytosolic functions. *Journal of cell science* **125**, 2815-2824, (2012).

- 43 Lindaman, L. L., Yeh, D. M., Xie, C., Breen, K. M. & Coss, D. Phosphorylation of ATF2 and interaction with NFY induces c-Jun in the gonadotrope. *Molecular and cellular endocrinology* **365**, 316-326, (2013).
- 44 Nogueira, E. F. & Rainey, W. E. Regulation of aldosterone synthase by activator transcription factor/cAMP response element-binding protein family members. *Endocrinology* **151**, 1060-1070, (2010).
- 45 Mynard, V. *et al.* Synergistic signaling by corticotropin-releasing hormone and leukemia inhibitory factor bridged by phosphorylated 3',5'-cyclic adenosine monophosphate response element binding protein at the Nur response element (NurRE)-signal transducers and activators of transcription (STAT) element of the proopiomelanocortin promoter. *Molecular endocrinology* **18**, 2997-3010, (2004).
- 46 Kodama, S., Moore, R., Yamamoto, Y. & Negishi, M. Human nuclear pregnane X receptor cross-talk with CREB to repress cAMP activation of the glucose-6-phosphatase gene. *The Biochemical journal* **407**, 373-381, (2007).
- 47 Mandlekar, S., Yu, R., Tan, T. H. & Kong, A. N. Activation of caspase-3 and c-Jun NH2-terminal kinase-1 signaling pathways in tamoxifen-induced apoptosis of human breast cancer cells. *Cancer research* **60**, 5995-6000, (2000).
- 48 Zhang, C. C. & Shapiro, D. J. Activation of the p38 mitogen-activated protein kinase pathway by estrogen or by 4-hydroxytamoxifen is coupled to estrogen receptor-induced apoptosis. *The Journal of biological chemistry* **275**, 479-486, (2000).
- 49 Buck, M. B., Pfizenmaier, K. & Knabbe, C. Antiestrogens induce growth inhibition by sequential activation of p38 mitogen-activated protein kinase and transforming growth factor-beta pathways in human breast cancer cells. *Molecular endocrinology* **18**, 1643-1657, (2004).
- 50 Ellis, M. J. & Perou, C. M. The genomic landscape of breast cancer as a therapeutic roadmap. *Cancer discovery* **3**, 27-34, (2013).

Supplementary Materials and Methods

Nucleic acid isolation

RNA was isolated using RNeasy mini-kit as per manufacturer's protocol (Qiagen, Venlo, The Netherlands), and for clinical samples total RNA was extracted from 10 μ m sections of formalin-fixed paraffin-embedded tissue following microdissection using the Recover All Total Nucleic Acid Isolation kit (Ambion, Foster City, USA).

RT-PCR analysis

cDNA was prepared using cDNA prep kit from ThermoScientific (Fermentas Life Sciences, York, UK). Amplification and analysis were done according to the manufacturer's protocol in 96 well plates in an ABI PRISM 7000 Sequence Detection System (Applied Biosystems, Foster City, USA) and the pre-cast "TaqMan® Gene Expression Assays" (Applied Biosystems, Foster City, USA). Quantification of target transcripts was performed in comparison to the reference transcript β 2-microglobulin (Hs99999907_m1), implementing the "delta-delta Ct method for comparing relative expression results in real-time PCR.

Flow cytometry

Cells were trypsinised, centrifuged at 1100 rpm for 5 minutes and re-suspended in 5 ml of ice-cold PBS, centrifuged as above, gently re-suspended in 2 ml ice-cold 70% ethanol and incubated at 4°C for one hour. Cells were washed twice with 5 ml of ice-cold PBS and re-suspended in 100 μ l of PBS containing 100 μ g/ml RNase (Sigma-Aldrich, UK) and 1ml of 50 μ g/ml propidium iodide (Sigma-Aldrich, UK) in PBS. Following incubation overnight in the dark at 4°C and filtering through 70 μ m muslin gauze into FACS tubes (Becton-Dickinson, UK) to remove cell clumps, stained cells were acquired using the RXP cytomics software on a Beckman Coulter Elite ESP (Beckman Coulter, High Wycombe, United Kingdom) and data were analysed using Flow Jo v7.2.5 (Tree Star Inc., San Carlos, CA).

Anchorage-Independent Soft Agar Growth Assay

One percent of soft agar gel-I (SA-I) was made from 2% low melting temperature agarose (LMA) mixed with equal amount of routine medium for siRNA transfected cells while 1% of soft agar gel-II (SA-II) was made from 2% LMA mixed with equal amount of DMEM-PR and 5% DSS with 100nM tamoxifen for siRNA transfected cells with antibiotic. SA-I and SA-II were plated at 2ml per well in a 6-well plate and placed at 4°C to solidify the basement gel layer. Untransfected, control and siRNA transfected MCF-7

were harvested separately, adjusted with SA-I or SA-II to 1×10^4 cells/ml, plated on top of the pre-set basement gel layer and placed at 4°C for 10 minutes for solidification. Once set, the cells in plates were incubated at 37°C in a humidified atmosphere of 5% CO_2 for 21 days. All soft agar gels were stained with 5% MTT for 4 hours. Plates were scanned and the colonies were counted using an Optronix Gel Count (Oxford Optronix, UK).

Chromatin Immunoprecipitation and Solexa sequencing (ChIP-Seq)

Chromatin Immunoprecipitations (ChIP) were performed as described previously¹. For each Chromatin Immunoprecipitation, 10mg of antibody and 100ml of Protein A magnetic beads was used (Invitrogen, Paisley, UK). The antibodies used were raised against ATF-2, and phospho-ATF-2 (Thr71), as previously described.

ChIP DNA was amplified as described¹. DNA was sequenced using the Illumina HiSeq 2000 genome analyser (using 50 bp reads), and aligned to the Human Reference Genome (assembly hg19, February 2009). Enriched regions of the genome were identified by comparing the ChIP samples to an input sample using the Model-based Analysis of ChIP-Seq (MACS) peak caller² version 1.3.7.1. Only peaks shared by both ATF-2 and phospho-ATF-2 were considered. Details of the number of reads obtained and the percentage of reads aligned, number of peaks called can be found in supplementary Table S4.

Motif analysis, heatmaps and genomic distributions of binding events

The genomic distributions of binding sites were analysed using the cis-regulatory element annotation system (CEAS)³. The genes closest to the binding site on both strands were analysed. If the binding region is within a gene, CEAS software indicates whether it is in a 5'UTR, a 3'UTR, a coding exon, or an intron. Promoter is defined as 3 kb upstream from RefSeq 5' start. If a binding site is further away than 3kb from a transcription start site, the peak is considered distal intergenic. For integration with gene expression data, binding events were considered proximal when identified in a gene body or within 20kb upstream of the transcription start site. Proximal enriched genes were analysed using Ingenuity Pathway Analysis software. Heatmaps were generated using Seqminer⁴ and Java Treeview (<http://jtreeview.sourceforge.net>), using default settings.

ChIP-qPCR Primers

Primer set	DNA region	Primer sequences	Position
1	chr1:59,249,762-59,249,907	(FW) CCCCTAAAAATAGCCCATGA (RV) CATTACCTCATCCCGTGAGC	Jun Promoter
2	chr3:156,530,423-156,530,551	(FW) CCCTGCAGGAGTTGGACTA (RV) TTTCCCTTCCCTGTTGCTAA	gene body LINC00886
3	chr7:104,653,473-104,653,602	(FW) CCATCGTCACTTCTCCCTCT (RV) AATCAGCGCCTGATGTGTC	gene body NR_024586 / KMT2E promoter
4	chr21:43,099,206-43,099,308	(FW) CCCCCTTGCAATGTGACTTA (RV) CATTCTATTGGCCATCGTGA	LINC00111 promoter
Ctrl (-)	chr1:17,079,211-17,079,290	(FW) CAGGATATACACCCCGTGA (RV) CAAAGTGCGTACACCTTGGTA	
(-)	chr11:69573441-69573595	(FW) TGGCCCTTGATACTGGAGTC (RV) GACATCCAAGGCAAGATGGT	

(-) = Enrichment of primer sites are relative to this negative region (position where ATF2 does not bind)

Clinical Breast Cancer Specimens**Paired Primary and Secondary Breast Cancers**

All cases were histologically confirmed as breast carcinoma. Where necessary, tumour was enriched by micro-dissection using sections stained with haematoxylin and eosin to identify areas of normal tissue. As normal tissue controls, RNA isolated from five pooled normal breasts obtained at reduction mammoplasty were utilised.

Nottingham Tenovus Primary breast cancer Series:

The Nottingham Tenovus Primary Breast Carcinoma Series is a well-characterised cohort comprised of women under the age of 71 years (median, 55 years), who were diagnosed between 1986 and 1999, with all patients being treated in a uniform way in a single institution. Information is available on the patients' clinical and pathological data including histological tumour type, primary tumour size, lymph node status, histological grade and data on other relevant biomarkers⁵.

Patients within the good prognosis group Nottingham Prognostic Index (NPI) ≤ 3.4 did not receive adjuvant therapy. Endocrine therapy was prescribed to patients with ER positive tumors and NPI scores >3.4 (moderate and poor prognostic groups). Pre-menopausal patients within the moderate and poor prognosis groups were candidates for chemotherapy. Conversely, ER positive postmenopausal patients with moderate or poor NPI were offered hormonal therapy, while ER negative patients received chemotherapy. Clinical data were maintained on a prospective basis with a median follow-up of 126 months (4-247).

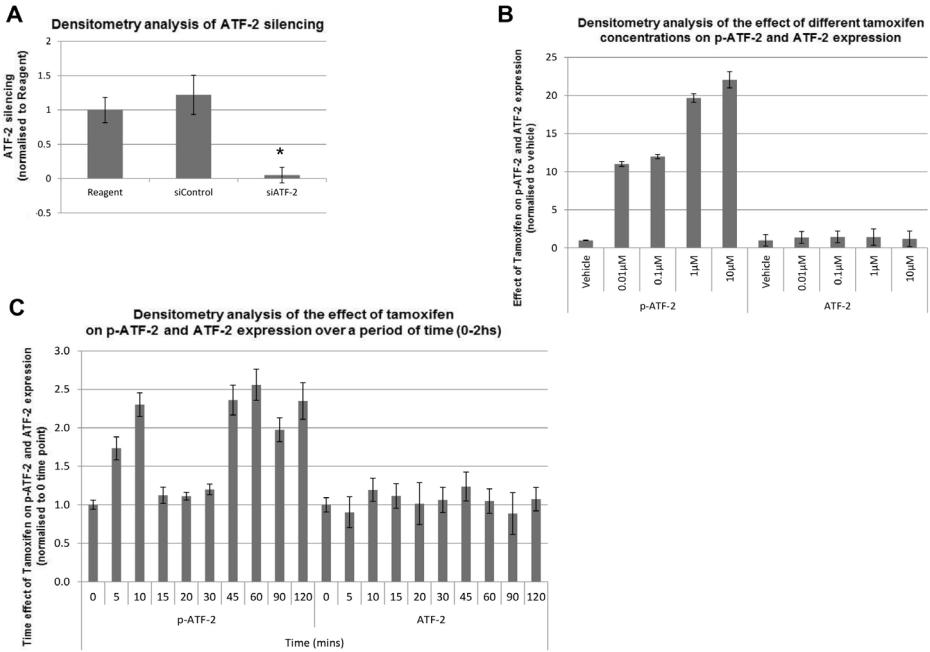
Statistical analysis

Survival data including survival time, disease-free survival (DFS), and development of loco-regional and distant metastases (DM) were maintained on a prospective basis. DFS was defined as the number of months from diagnosis to local recurrence, local lymph node (LN) relapse or DM relapse. Breast cancer specific survival (BCSS) was defined as the number of months from diagnosis to the occurrence of BC related-death. Local recurrence survival (LRS) was defined as the number of months from diagnosis to the occurrence of local recurrence. DM-free survival was defined as the number of months from diagnosis to the occurrence of DM relapse. Survival was censored if the patient was still alive, lost to follow-up, or died from other causes.

References

- 1 Schmidt D, Wilson MD, Spyrou C, Brown GD, Hadfield J, Odom DT. ChIP-seq: using high-throughput sequencing to discover protein-DNA interactions. *Methods*. 2009;48:240-8.
- 2 Zhang Y, Liu T, Meyer CA, Eeckhoute J, Johnson DS, Bernstein BE, et al. Model-based analysis of ChIP-Seq (MACS). *Genome Biol*. 2008;9:R137.
- 3 Ji X, Li W, Song J, Wei L, Liu XS. CEAS: cis-regulatory element annotation system. *Nucleic Acids Res*. 2006;34:W551-4.
- 4 Ye T, Krebs AR, Choukrallah MA, Keime C, Plewniak F, Davidson I, et al. seqMINER: an integrated ChIP-seq data interpretation platform. *Nucleic Acids Res*. 2011;39:e35.
- 5 Abdel-Fatah TM, Powe DG, Ball G, Lopez-Garcia MA, Habashy HO, Green AR, et al. Proposal for a modified grading system based on mitotic index and Bcl2 provides objective determination of clinical outcome for patients with breast cancer. *J Pathol* 2010; 222: 388-99.

Supplementary Figures and Tables

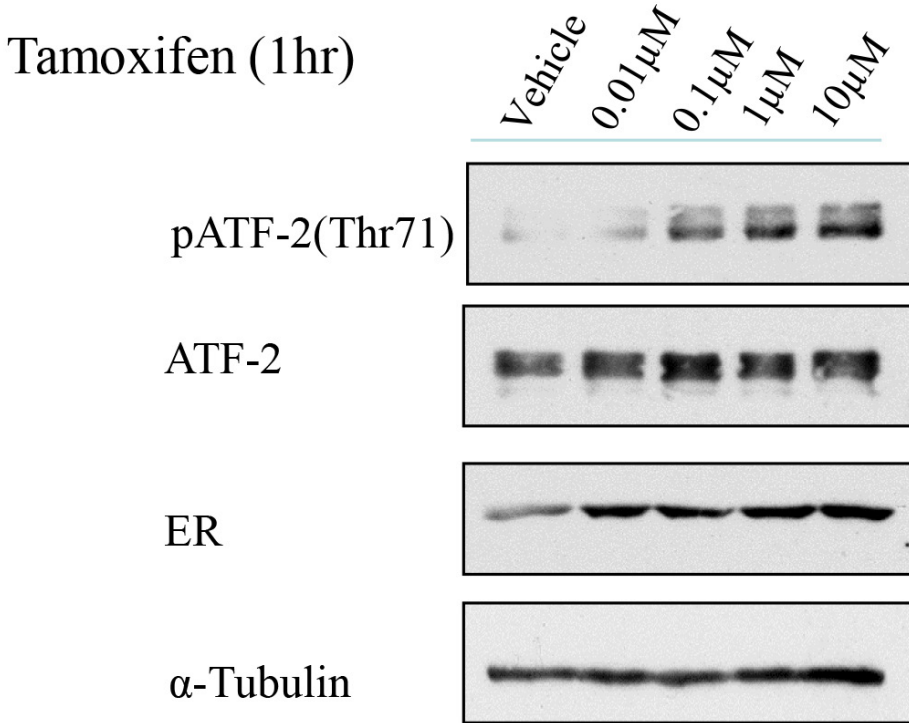


Supplementary Figure S1. Densitometry analysis of silenced ATF-2 and effects on growth of MCF-7, sensitivity to tamoxifen and modulation of ATF-2 phosphorylation at pATF-2-Thr69/71 by tamoxifen

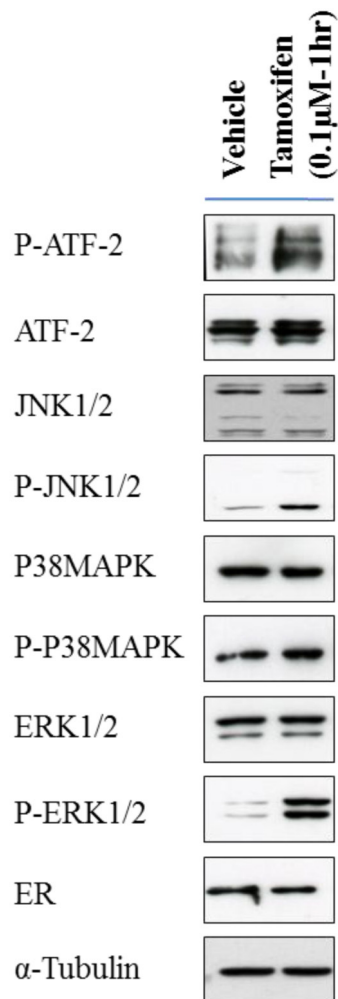
A) Corresponding densitometry analysis of Figure 1A: ATF-2 silencing versus control silencing ($p=0.00052$, $n=3$)

B) Corresponding densitometry analysis of Figure 2A: 1h treatment with tamoxifen leads to increased p-ATF-2 but no changes to total ATF-2.

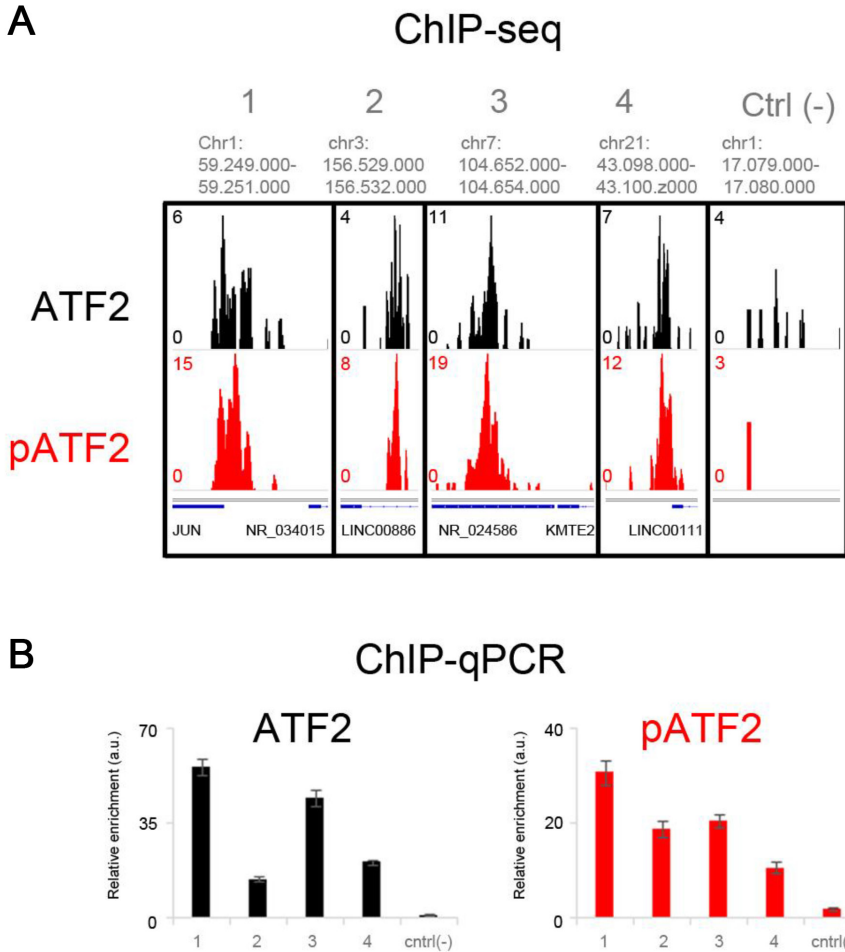
C) Corresponding densitometry analysis of Figure 2B: Time course assay (0-2hs) showing the effect of 0.1 μ M tamoxifen on p-ATF-2 and total ATF-2.



Supplementary Figure S2. Modulation of ATF-2 phosphorylation by tamoxifen
Exponentially growing MCF-7 cells in their basal media were treated with either ethanol (vehicle) or for 1hr with indicated concentration of tamoxifen. Cells were harvested for immunoblotting and probed with indicated antibodies. Tubulin was used as loading control. Results are representative of three independent experiments.



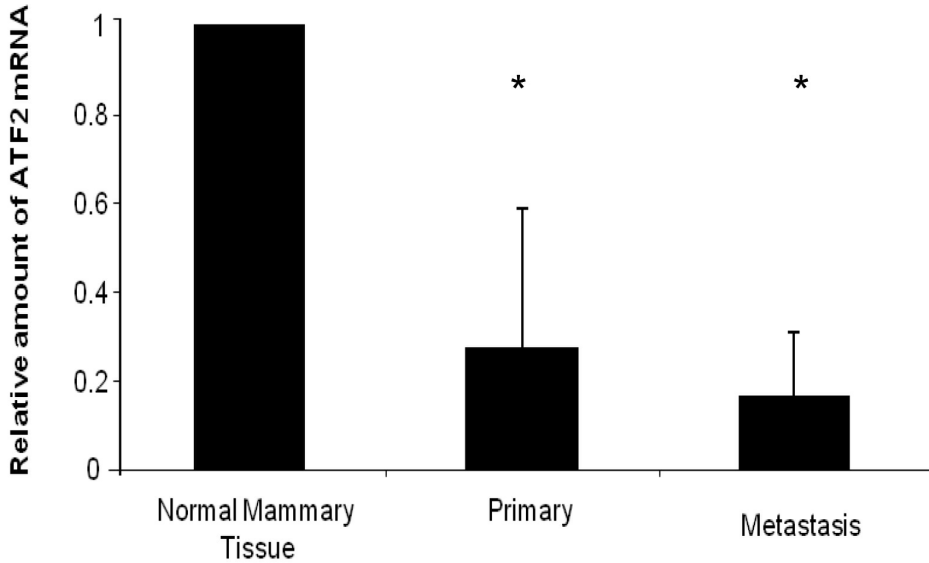
Supplementary Figure S3. Tamoxifen stimulates downstream kinases MCF-7 cells growing in basal media were treated with either vehicle or tamoxifen or for 1hr. Cells were harvested for immunoblotting and probed with indicated total and phospho-antibodies. Tubulin was used as loading control. Results are representative of three independent experiments.



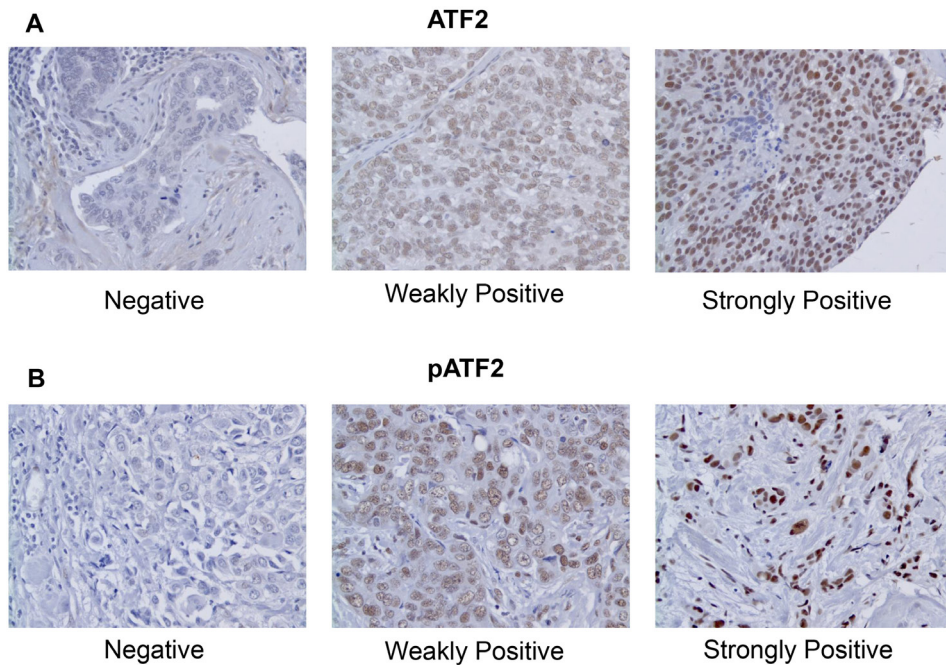
Supplementary Figure S4. ChIP shows that ATF-2 binds the chromatin in the presence of tamoxifen.

A) Genome-browser snapshot of total ATF-2 (black) and phosphorylated ATF-2 (red) binding to chromatin in MCF7 in the presence of tamoxifen. Genomic locations are depicted above and total reads are shown on the y-axis per region.

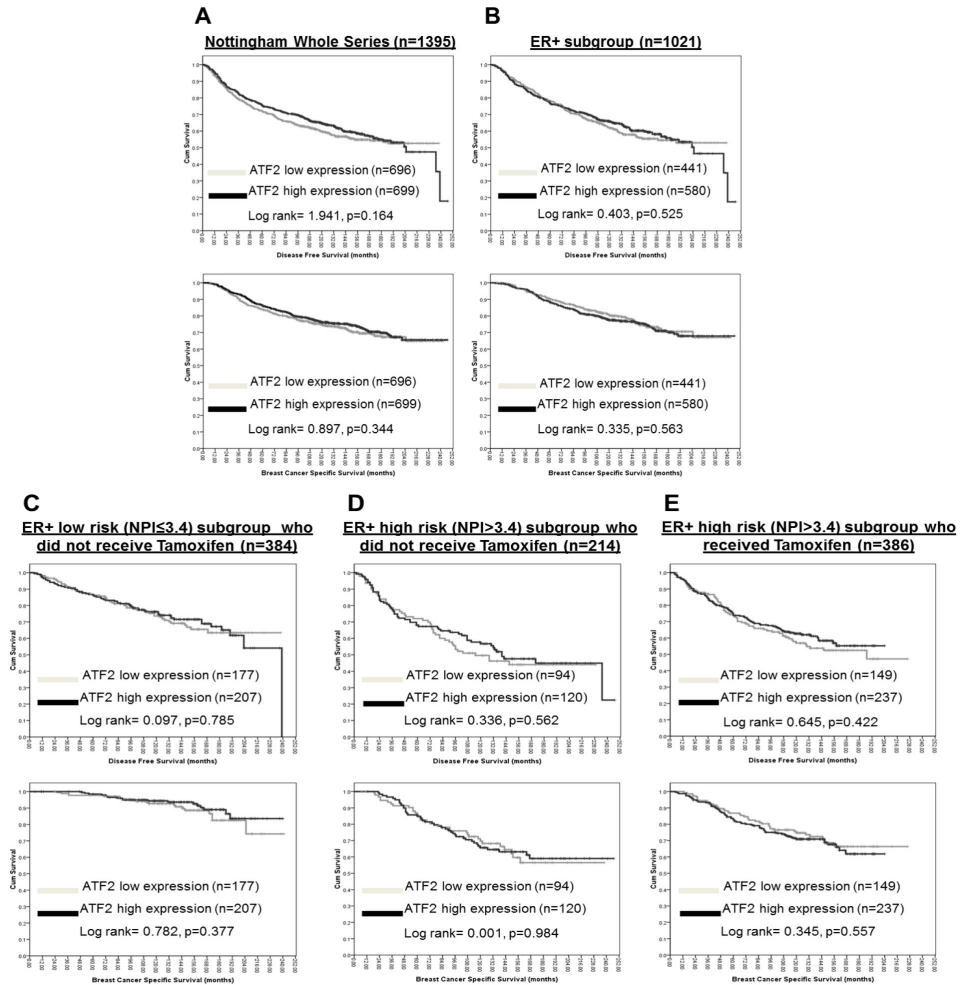
B) ChIP-qPCR of genomic regions corresponding to those shown in A. Enrichment is relative to a negative region. A second negative control is shown by Ctrl (-). Error bars represent technical triplicate.



Supplementary Figure S5. ATF-2 expression and amplification in human breast cancer qPCR analysis of ATF-2 expression in normal (n=5) and paired primary and metastatic breast cancer samples (n=20). cDNA was prepared and expression of ATF-2 mRNA determined as described in Methods. Expression is shown as means \pm standard deviation of primary and metastatic tumours compared to normal mammary tissues. * $p < 0.05$ (vs control).



Supplementary Figure S6. ATF-2 and pATF-2- Thr71 Immunohistochemistry
A) Photomicrographs of immunohistochemical staining in breast carcinoma showing negative, weak and strongly positive nuclear ATF-2 protein expression. Original magnification, x400.
B) Photomicrographs of immunohistochemical staining in breast carcinoma showing negative, weak and strongly positive nuclear pATF-2. Original magnification, x400.



4

Supplementary Figure S7. Kaplan-Meier survival curve ATF-2 Kaplan-Meier survival curve showing percentage disease free survival (DFS) and breast cancer specific survival (BCSS) with and without tamoxifen of patients with ATF-2 overexpressing tumours compared with all other patients for:

- A)** Entire Nottingham cohort.
- B)** ERa positive Cohort.
- C)** ERa positive patients NPI <3.4 who did not receive tamoxifen.
- D)** ERa positive patients NPI >3.4 who did not receive tamoxifen.
- E)** ERa positive patients NPI >3.4 who received tamoxifen.

Supplementary Table S1. Genes with proximal pATF-2 binding

#chrom	gTSS	gTTS	gene
chr1	107599266	107601907	PRMT6
chr1	107682628	108024471	NTNG1
chr1	112318453	112531777	KCND3
chr1	114437676	114447741	AP4B1
chr1	114447914	114456707	DCLRE1B
chr1	114471995	114514693	HIPK1
chr1	114935400	115053781	TRIM33
chr1	115110182	115124265	BCAS2
chr1	115127195	115212732	DENND2C
chr1	115215721	115238239	AMPD1
chr1	115247078	115259515	NRAS
chr1	115259537	115300624	CSDE1
chr1	115312106	115323308	SIKE1
chr1	120454177	120612276	NOTCH2
chr1	144480747	144521969	LOC728875
chr1	144951760	144995033	PDE4DIP
chr1	145096406	145116922	SEC22B
chr1	145209110	145285911	NOTCH2NL
chr1	145293370	145368682	NBPF10
chr1	145470507	145475647	ANKRD34A
chr1	145438461	145442626	TXNIP
chr1	145456235	145470387	POLR3GL
chr1	145477084	145499090	LIX1L
chr1	148577356	148596267	NBPF16
chr1	148558187	148596267	NBPF15
chr1	150521897	150533410	ADAMTSL4
chr1	150547036	150552136	MCL1
chr1	150524404	150524490	MIR4257
chr1	150594603	150602098	ENSA
chr1	152004982	152009511	S100A11
chr1	201979689	201986306	ELF3
chr1	202163117	202288888	LGR6
chr1	228780656	228788159	DUSP5P
chr1	31885962	31907524	SERINC2
chr1	566188	566265	MIR1977
chr1	59246463	59249785	JUN
chr1	59250822	59365384	LOC100131060
chr1	700244	714068	LOC100288069

chr1	91726323	91870426	HFM1
chr1	14362	29370	WASH7P
chr1	34611	36081	FAM138A
chr1	34611	36081	FAM138F
chr1	34611	36081	FAM138C
chr10	127524908	127569884	DHX32
chr10	127585107	127698159	FANK1
chr10	135480367	135485275	DUX4L2
chr10	135480370	135485275	DUX4L7
chr10	135480370	135485275	DUX4L6
chr10	135480370	135485275	DUX4L5
chr10	135480370	135485275	DUX4L3
chr10	135480368	135485275	DUX4
chr10	52065345	52383737	SGMS1
chr11	10529435	10530723	MTRNR2L8
chr11	3659735	3663546	ART5
chr11	3666360	3685646	ART1
chr11	3686817	3692614	CHRNA10
chr11	3647713	3658789	TRPC2
chr11	55029657	55038594	TRIM48
chr11	560970	564024	RASSF7
chr11	576482	612220	PHRF1
chr11	554850	560779	C11orf35
chr11	573808	575885	LOC143666
chr11	568088	568198	MIR210
chr12	121866901	122018364	KDM2B
chr12	65277553	65371301	FLJ41278
chr12	87983	91262	LOC100288778
chr13	28009775	28024334	MTIF3
chr14	38059192	38064489	FOXA1
chr14	50044052	50053094	RPS29
chr14	50065414	50081389	PPIL5
chr14	77787705	77797939	GSTZ1
chr14	77741298	77787225	POMT2
chr14	90921573	90925248	LOC400238
chr15	52484516	52587995	MYO5C
chr15	52569314	52569397	MIR1266
chr15	83517737	83621473	HOMER2
chr15	83654994	83659423	FAM103A1
chr15	91509273	91537804	PRC1

chr15	91541773	91565833	VPS33B
chr16	33298268	33298702	LOC390705
chr16	33965507	33965592	MIR1826
chr17	33458367	33469322	NLE1
chr17	33474835	33516363	UNC45B
chr17	33448630	33457750	FNDC8
chr17	41363893	41371589	TMEM106A
chr17	41476352	41478503	ARL4D
chr17	41447212	41466266	LOC100130581
chr17	55940336	55980750	CUEDC1
chr17	56078281	56084707	SRSF1
chr17	56431039	56494931	RNF43
chr17	57297827	57353325	GDPD1
chr17	57287370	57292610	C17orf71
chr17	57642885	57685712	DHX40
chr17	57697049	57774317	CLTC
chr17	57774667	57784856	PTRH2
chr17	57784862	57917950	TMEM49
chr17	59942728	60005377	INTS2
chr17	60019966	60142643	MED13
chr17	60342068	60353016	TBC1D3P2
chr17	60501245	60527454	METTL2A
chr17	60556385	60692839	TLK2
chr17	60798857	61268734	MIR548W
chr17	60778675	60884011	10-Mar
chr17	61086897	61505066	TANC2
chr17	61509665	61523545	CYB561
chr17	61780193	61819330	STRADA
chr17	61851566	61896676	DDX42
chr17	61822610	61851088	CCDC47
chr17	61909440	61920351	SMARCD2
chr17	61904809	61909386	PSMC5
chr17	61896794	61905031	FTSJ3
chr17	61934375	61941738	TCAM1P
chr17	62120389	62207502	ERN1
chr17	62223698	62223830	SNORA76
chr17	62223437	62223517	SNORD104
chr17	62399863	62401205	PECAM1
chr17	62540734	62658386	SMURF2
chr17	63524684	63557740	AXIN2

chr17	64961012	65029518	CACNG4
chr17	65040705	65052909	CACNG1
chr17	73314157	73401789	GRB2
chr17	73452663	73496530	KIAA0195
chr17	73754018	73761280	GALK1
chr17	73780680	73821885	UNK
chr17	73772516	73775860	H3F3B
chr17	74536120	74541458	PRCD
chr17	74523439	74533782	CYGB
chr17	74557714	74557788	SNORD1A
chr17	74557189	74557275	SNORD1B
chr17	74554873	74554951	SNORD1C
chr17	81037566	81052589	METRNL
chr18	109064	122217	ROCK1P1
chr18	32073253	32409292	DTNA
chr18	3262610	3278280	MYL12B
chr18	3247527	3256228	MYL12A
chr19	36041094	36054560	ATP4A
chr19	36036544	36038428	TMEM147
chr19	42751717	42759309	ERF
chr19	42788816	42799949	CIC
chr19	42734337	42746736	GSK3A
chr19	44889808	44905777	ZNF285
chr19	50595745	50595866	SNAR-A3
chr19	50595745	50595866	SNAR-A4
chr19	50595745	50595866	SNAR-A5
chr19	50595745	50595866	SNAR-A7
chr19	50595745	50595866	SNAR-A11
chr19	50595745	50595866	SNAR-A9
chr19	50595745	50595866	SNAR-A6
chr19	50595745	50595866	SNAR-A8
chr19	50595745	50595866	SNAR-A10
chr19	50595745	50595866	SNAR-A14
chr2	132905163	133015542	ANKRD30BL
chr2	133014538	133014653	MIR663B
chr2	149632818	149883273	KIF5C
chr2	149639364	149639417	MIR1978
chr2	162164785	162268226	PSMD14
chr2	192110106	192290115	MYO1B
chr20	29611878	29634007	FRG1B

chr20	29845466	29847435	DEFB115
chr20	48519930	48530276	SPATA2
chr20	48552913	48570420	RNF114
chr20	48697662	48729710	UBE2V1
chr20	48740273	48770335	TMEM189
chr20	48697662	48770335	TMEM189-UBE2V1
chr20	48807375	48809212	CEBPB
chr20	49126890	49201084	PTPN1
chr20	50213313	50384908	ATP9A
chr20	55904830	55919048	SPO11
chr20	55896557	55896647	MIR4325
chr20	56223453	56285031	PMEPA1
chr20	62271060	62284780	STMN3
chr20	62289646	62327597	RTEL1
chr20	62326287	62330033	TNFRSF6B
chr21	11057795	11098937	BAGE
chr21	11020841	11098925	BAGE4
chr21	11020841	11098925	BAGE3
chr21	11020841	11098925	BAGE2
chr21	11020841	11098925	BAGE5
chr21	39426313	39493454	DSCR4
chr21	39493544	39528604	DSCR8
chr21	43099461	43117496	NCRNA00111
chr22	18893735	18899600	DGCR6
chr22	20301760	20307628	DGCR6L
chr3	156544095	156763918	LEKR1
chr3	156527059	156529810	PA2G4P4
chr3	62305395	62319318	C3orf14
chr3	63638343	63650881	SNTN
chr4	53276	156488	ZNF718
chr4	53226	88099	ZNF595
chr4	80238272	80247171	NAA11
chr5	134240809	134298335	PCBD2
chr5	172195094	172198203	DUSP1
chr5	79922044	79950800	DHFR
chr5	79945820	79946854	MTRNR2L2
chr5	79950293	80172633	MSH3
chr6	21593971	21598847	SOX4
chr6	26216427	26216872	HIST1H2BG
chr6	26199786	26200215	HIST1H2BF

chr6	26184023	26184457	HIST1H2BE
chr6	26197012	26199464	HIST1H3D
chr6	26225382	26225843	HIST1H3E
chr6	26188938	26189304	HIST1H4D
chr6	26204872	26205248	HIST1H4E
chr6	26217147	26217711	HIST1H2AE
chr6	26199012	26199471	HIST1H2AD
chr7	104654636	104754531	MLL5
chr7	104650988	104654588	LOC100216545
chr7	107384278	107402082	CBLL1
chr7	157331750	158380482	PTPRN2
chr8	102504667	102681950	GRHL2
chr8	128806778	129113498	PVT1
chr8	128808207	128808274	MIR1204
chr8	129162361	129162434	MIR1208
chr8	144766621	144777554	ZNF707
chr8	144731953	144735900	ZNF623
chr8	144779284	144780582	BREA2
chr8	80947104	80993010	TPD52
chr8	82711819	82754521	SNX16
chr8	86568694	86575726	REXO1L1
chr8	86566827	86567905	REXO1L2P
chr9	140194082	140196703	NRARP
chr9	44990235	44991491	FAM27C
chr9	67270214	67289492	AQP7P1
chr9	67792929	67794189	FAM27B
chr9	68427782	68454375	LOC642236
chr9	72658496	72841888	MAMDC2
chrX	281384	282052	NCRNA00107

Supplementary Table S2: Clinico-pathological characteristics of Nottingham Tenovus Primary breast cancer series.

Variable	Pathological Parameters:	N (%)
ATF-2 expression (n=1388)	Low	689 (49.6)
	High	699 (50.4)
pATF-2 expression (n=1516)	Low	680 (44.9)
	High	836 (55.1)
Tumour size (n=1625)	T1 a+ b (≤ 1.0)	176 (10.8)
	T1 c ($>1.0-2.0$)	818 (50.3)
	T2 ($>2.0-5.0$)	590 (36.3)
	T3 (>5)	41 (2.5)
Lymph node stage (n=1632)	Negative	1014 (62.1)
	Positive (1-3 nodes)	474 (29)
	Positive (>3 nodes)	144 (8.8)
Tumour grade (n=1625)	Low grade (G1)	284 (17.5)
	Intermediate grade (G2)	544 (33.5)
	High grade (G3)	797 (49)
Lymphovascular invasion (n=1607)	No	1100 (68.5)
	Yes	507 (31.5)
Tumour type (n= 1390)	IDC-NST	807 (58.1)
	Medullary	32 (2.3)
	Tubular	285 (20.5)
	Lobular	147 (10.6)
	Others	119 (8.6)
Mitotic index (n=1611)	M1 (low; mitoses <10)	597 (37.1)
	M2 (medium; mitoses 10-18)	291 (18.1)
	M3 (high; mitoses >18)	723 (44.9)
Bilateral phenotype (n=1398)	Unilateral	1338 (95.7)
	Bilateral	60 (4.3)
Oestrogen receptor (n=1596)	Negative	417 (26.1)
	Positive	1179 (73.9)
HER2 receptor (n=1592)	Negative	1418 (89.1)
	Overexpression	174 (10.9)
Triple negative phenotype (1580)	No	1291 (81.7)
	Yes	289 (18.3)
Basal like phenotype (n=1545)	No	1363 (88.2)
	Yes	182 (11.8)

Supplementary Table S3: Interaction between tamoxifen and pATF-2- Thr71 in ER positive/high risk (NPI>3.4) patients.

Breast cancer specific survival				Disease Free Survival				
Variables	HR	95% CI		P	HR	95% CI		P
		Lower	Upper			Lower	Upper	
Univariate analysis(Crude)								
pATF-2-T71	0.716	0.543	0.944	0.018	0.762	0.604	0.961	0.022
Tamoxifen	0.791	0.605	1.034	0.087	0.641	0.517	0.795	0.00005
pATF-2-T71*Tamoxifen (interaction)	0.80	0.668	0.95	0.011	0.786	0.678	0.910	0.001
Multivariate analysis (Adjusted)								
pATF-2-T71	0.693	0.519	0.925	0.013	0.757	0.596	0.962	0.023
Tamoxifen	0.797	0.591	1.075	0.137	0.731	0.570	0.937	0.014
Interaction test								
pATF-2-T71	0.723	0.535	0.978	0.035	0.776	0.605	0.996	0.047
Tamoxifen	0.784	0.580	1.095	0.113	0.726	0.566	0.932	0.012
pATF-2-T71*Tamoxifen (interaction)	0.727	0.398	1.328	0.300	0.835	0.507	1.375	0.439

Supplementary Table S4: Culture conditions and read count for ChIP-seq experiments.

ChIP condition	cell line	treatment	read count	mapped reads	% mapped
ATF-2	MCF-7	1 hr 4OH-tamoxifen	6575235	6395296	97
phospho-ATF-2	MCF-7	1 hr 4OH-tamoxifen	13976182	13304380	95

